Numerical Simulations of Conservation Laws in Random Heterogeneous Media

by

Baris Kopruluoglu

A dissertation submitted to the Graduate Faculty of
Auburn University
in partial fulfillment of the
requirements for the Degree of
Doctor of Philosophy

Auburn, Alabama
August 8, 2020

Keywords: Conservation Laws, Random Media, Stochastic Finite Volume Method, Monte Carlo Finite Volume Method

Approved by

Hans Werner van Wyk, Chair, Assisstant Professor of Mathematics and Statistics
Yanzhao Cao, Professor of Mathematics and Statistics
Erkan Nane, Associate Professor of Mathematics and Statistics
Bertram Zinner, Associate Professor of Mathematics and Statistics
George Flowers, Dean of the Graduate School and Professor in Mechanical Engineering

Abstract

Conservation laws play an important role in many areas of natural science. When we design numerical schemes for conservation laws, we usually assume that initial data and flux function (the rate of change of quantity of interest) are known exactly. However, this is generally not the case as these are often obtained through indirect measurements. As a consequence the initial data and flux function are known only in terms of statistical quantities like mean, variance and involve some uncertainty. These uncertain inputs should be handled statistically. In our study, we analyze and implement the Monte Carlo Finite Volume Method and the Stochastic Finite Volume Method to solve conservation laws in random media. We particularly focus on Stochastic Finite Volume Method and formulate an algorithm for conservation laws with random initial data. Our simulations include that of the inviscid Burgers equation with random inputs.

Acknowledgments

I would like to thank my advisor Dr. Hans Werner van Wyk for his huge support. He has been always encouraging, helpful and patient with me. I wouldn't been able to complete my dissertation without his help. I will always remember his contribution to my research studies and be grateful. I am very grateful for my family and friends for always believing in me and supporting me. Also, I want to thank Dr. Yanzhao Cao, Dr. Erkan Nane and Dr. Bertram Zinner for being in my committee and thank Dr. Chandana Mitra for joining the committee as university reader.

Contents

List of Figures

Chapter 1

Introduction

1.1 Conservation Laws

Many wave motion problems in Natural Science are modeled by a first order hyperbolic partial differential equation. In particular, conservation and balance laws are used to describe wave and advection phenomena in a variety of settings ranging from gas dynamics, modeled by the Euler equations, to ocean waves, modeled by the shallow water equations. The general form of balance Laws is given as follows [3]:

$$\begin{cases} \partial_t U + \nabla_x \cdot F = S \\ U(x,0) = U_0(x) \end{cases} \tag{1.1}$$

where

- U is the vector of conserved quantity, $U = U(x,t) : \mathbb{R}^d \times \mathbb{R}_+ \to \mathbb{R}^m$
- F is the flux function, $F = F(U) = (F^1, ..., F^d) : \mathbb{R}^m \to \mathbb{R}^{m \times d}$
- S is the source term, $S = S(x,t,U) : \mathbb{R}^d \times \mathbb{R}_+ \times \mathbb{R}^m \to \mathbb{R}^m$

This phenomenological observation can be interpreted as: The sum of the time rate of change of conserved quantity U in any fixed domain and the flux of U across the boundary of the domain equals U produced or used inside the domain (source). The special case, $S = 0$ is called *conservation law* as the only change in U comes from the quantity entering or leaving the domain of interest. In particular, when $m = 1$, System (1.1) is called *scalar conservation law*.

Characteristics of such systems include waves with finite propagation speed and formation of shocks. In fact, the solutions of (1.1) can involve discontinuities even if the initial data is smooth, thus the solutions must be sought in "weak" sense. The issue with the weak solutions is that they are not unique. To obtain uniqueness when $d > 1$ and $N = 1$ (scalar case), an entropy condition is necessary [2]. The weak solution satisfying an entropy condition is called *entropy solution* which will be introduced in Chapter 3. The numerical methods to approximate entropy solutions have been frequently applied. In particular, finite volume methods have been employed to approximate entropy solutions [59] , [61]. The reason why finite volume methods are more preferable than finite element methods to solve conservation laws is that they are more able to capture the shocks in the solutions. Godunov, Engquist-Osher, Rusanov, Lax Friedrichs methods are some of the well-known finite volume methods to solve (1.1) *deterministic conservation laws* (the case without randomness).

The main assumption when a numerical scheme is designed to solve conservation laws is that the initial data and flux function is known for certain. In general, these data are not exactly known and can be obtained in terms of statistical quantities of interest such as mean, variance and higher moments. In such cases, we need to reformulate the conservation law with random problem data. If we rewrite (1.1) with no source term and random inputs:

$$\begin{cases} \partial_t U(x,t,\omega) + \nabla_x \cdot F(U,\omega) = 0 \\ U(x,0,\omega) = U_0(x,\omega) \end{cases} \tag{1.2}$$

where ω is the random variable which represents the uncertainty. The system basically produces a sample path for each ω to reflect the uncertainty, then we compute its statistical quantities of all paths and this allows us to make predictions in more realistic scenarios. To numerically solve (1.2), there have been a lot of recent studies. The numerical methods including Monte-Carlo Finite Volume Method [9], [13] , Stochastic Collocation Method [43]

and Stochastic Finite Volume Method [1] have been developed to approximate entropy solution of random conservation laws. The existence and uniqueness of random entropy solutions for scalar conservation laws have been shown by Mishra and Schwab [13].

I will present some of the commonly used applications of conservation laws.

1.2 Examples of Conservation Laws

- Traffic Flow Problem [10]

  Let's consider a road starting at point a and ending at point b. Let $u(x,t)$ be the density of cars at point x , time t. Hence, the total number of cars between the points a and b can be shown as

$$\int_a^b u(x,t)dx$$

  At time t, the rate of change in the number of cars between a and b is given by

$$\frac{d}{dt}\int_a^b u(x,t) = f(u(a,t)) - f(u(b,t))$$

  where f represents the flow rate onto and off the street. Supposing that f and u are continously differentiable functions, we see that

$$\int_a^b u_t(x,t) = f(u(a,t)) - f(u(b,t))$$

  and, therefore,

$$\frac{1}{b-a}\int_a^b u_t(x,t) = \frac{f(u(a,t)) - f(u(b,t))}{b-a}$$

  then

$$\lim_{b\to a}\frac{1}{b-a}\int_a^b u_t(x,t) = \lim_{b\to a}\frac{f(u(a,t))-f(u(b,t))}{b-a}$$

so we obtain

$$u_t = -[f(u)]_x$$

Hence, it can be concluded that the density of cars at point x at time t satisfies the first order PDE also known as scalar conservation law:

$$u_t + [f(u)]_x = 0 \tag{1.3}$$

where f is a smooth function. However, this is assuming the density of cars is a continuous function. We aim to attain some sort of notion to say that a function u which is not even differentiable will "solve" the PDE.

(1.3) is the general form of scalar conservation laws which will be studied more detailed in Chapter 2.

- Euler Equations of Gas Dynamics [7]

  When the motion of the gas is modeled, it is difficult to track the motion of each molecule of gas individually, since gas consists of a huge number of molecules. Instead, a more macroscopic model can be used. The quantities of interest are the gas density, velocity field and gas pressure.

  Consider a tube that is filled with gas and assume that the initial position of the diaphragm is uncertain. The relevant conservation law can be written as :

$$u_t + (\rho u)_x = 0$$

where u is the gas density, ρ is the velocity field. To handle the unknown initial condition, we benefit from some prior knowledge about the field and can write

$$u(x,0) = \begin{cases} 1 \ if \ x \leq x_d \\ 0.125 \ else \end{cases}$$

we set $x_d = 0.5 + 0.05\omega$ where the stochastic parameter $\omega \in [-1,1]$ parametrizes a uniform law.

This is an example of conservation law with random initial data which will be explained more deeply in Chapter 3.

- Elastic Waves in Heterogeneous Media [24]

  Consider the propagation of compressional waves in heterogenous (spatially dependent) media in 1-D. The motion of waves in elastic rod with density $\rho(x)$, strain $\epsilon(x,t)$ and stress $\sigma(\epsilon,x)$ can modeled by kinematic relation and Newton's second law:

$$\begin{cases} \epsilon_t - u_x = 0, \\ m_t - \sigma_x = 0, \end{cases}$$

  where $m(x,t) = \rho(x)u(x,t)$ denotes momentum. This system can be written as a conservation law

$$q_t + f(q,x)_x = 0$$

  where

$$q(x,t) = \begin{bmatrix} \epsilon \\ \rho u \end{bmatrix} = \begin{bmatrix} \epsilon \\ m \end{bmatrix} \qquad f(x,t) = \begin{bmatrix} -m/\rho(x) \\ -\sigma(\epsilon,x) \end{bmatrix}$$

- Shallow Water Equation [11]

  The system of one-dimensional equations of shallow water theory, neglecting the effects of friction and inclination of the bottom, has the form of two quasilinear differential equations :

$$\begin{cases} h_t + vh_x + hv_x = 0 \\ v_t + gh_x + vv_x = 0 \end{cases}$$

  where $h = h(x,t)$ is the depth of the flow, $v = v(x,t)$ denotes the flow velocity over the cross section and g is the gravitational acceleration. This system can be rewritten as

$$u_t + A(u)u_x = 0, \qquad u = \begin{pmatrix} h \\ v \end{pmatrix}, \qquad A(u) = \begin{pmatrix} v & h \\ g & v \end{pmatrix}$$

  Let $U(u)$ and $F(u)$ satisfy the vector equation $U_u A(u)_u = F_u$. Then the system admits infititely many linear conservation laws:

$$[U(u)]_t + [F(u)]_x = 0$$

1.3 Outline of the Dissertation

This dissertation's main interest is to analyze the methods to produce numerical simulations for conservation laws in random media in one dimensional space, in particular conservation laws with random initial data.

First, the deterministic scalar case for Conservation Laws in 1-D will be analyzed in Chapter 2. The prototype for conservation laws Burger's equation will be introduced and the methods to solve deterministic inviscid Burger's equation, i.e. finite volume methods and a particular flux limiter method will be discussed. Some numerical experiments will be shown

and the efficiency of these methods will be stated.

In Chapter 3, the random conservation laws and the methods to solve random conservation laws in particular Burger's equation with random initial data will be discussed. I will mention the general numerical challenges to simulate random conservation laws. The algorithms, implementations, convergence analysis and work estimates for Monte Carlo Finite Volume Method and Stochastic Finite Volume Method will be presented. Stochastic Finite Volume Method will be focused on more detailed. I will show how its algorithm is obtained. How the methods for deterministic case are used to solve random conservation laws will be explained.

Chapter 2

Deterministic Conservation Laws

2.1 Burger's Equation

Let's consider a scalar one-dimensional conservation law:

$$u_t + f(u)_x = 0 \tag{2.1}$$

The scalar transport equation can be written as

$$u_t + a(x,t)u_x = 0 \tag{2.2}$$

where $a(x,t)$ is the velocity field. A special case is the linear advection(transport) equation where the velocity is constant $a(x,t) = a$. However, the most general and natural phenomena are nonlinear. In such models, the velocity field depends on the quantity u itself. The simplest nonlinear case is $a(x,t) = u(x,t)$ hence (2.2) becomes

$$u_t + uu_x = 0 \tag{2.3}$$

which is called *inviscid Burger's equation.* It can be rewritten in the conservative form

$$u_t + (\frac{u^2}{2})_x = 0 \tag{2.4}$$

Burger's equation serves as a prototype for scalar conservation laws where flux function $f(u) = \frac{u^2}{2}$. It is regarded as the simplest model for nonlinear advection and diffusion. I will mainly focus on inviscid Burger's equation in our applications.

2.1.1 Riemann problems for Burgers Equation

The characteristics $x(t)$ for Burger's equation ,when u is smooth, are given by

$$\begin{cases} x'(t) = u(x(t), t) \\ x(0) = x_0 \end{cases}$$

We consider the initial data

$$u_0(x) = \begin{cases} u_L \ \ if \ x < 0 \\ u_R \ \ if \ x > 0 \end{cases}$$

Data consists of piecewise constants seperated by a discontinuity of the origin. The initial value problem for a conservation law $u_t + f(u)_x = 0$ is called *Riemann problem*. The solution u does not vary along the characteristics, that is, $u(x(t), t) = u_0(x_0)$. Therefore, the characteristic solution is [5]

$$x(t) = u_0(x_0)t + x_0$$

One of the simplest choices for the Riemann problem is $u_L = 1$ and $u_R = 0$. For $x_0 < 0$, the characteristics will have velocity $u(x_0) = 1$, while for $x_0 > 0$ the velocity is 0. Hence, the characteristics will intersect immediately. It reveals that even smooth initial data can cause intersection of characteristics, so smooth solutions cannot be obtained. The formation of discontinuities in the solution of Burger's equation are expected. Therefore, the solutions have been interpreted in the weak sense. However, the weak solutions are not unique. The numerical methods for approximating entropy solutions of systems of Burger's equation have been extensively developed. One of the most commonly used numerical methods is finite volume methods.

2.2 Finite Volume Methods for Scalar Conservation Laws

2.2.1 Cell Averages

We want to capture the discontinuities occurring in the solution of conservation laws, hence finite volume methods are designed to numerically solve scalar conservation laws. Let's consider the uniform discretization of the spatial domain $[x_L, x_R]$. Hence the discrete points are obtained as $x_j = x_L + (j + 1/2)\Delta x$, for $j = 0, .., N$, where $\Delta x = \frac{x_R - X_L}{N+1}$. An uniform discretization in time with time step Δt will be used. The time levels are denoted by $t^n = n\Delta t$. Let's define the cell averages at each time level [5],

$$u_j^n \approx \frac{1}{\Delta x} \int_{x_{j-1/2}}^{x_{j+1/2}} u(x, t^n) dx$$

which is the main quantity of interest for our approximation. The aim of the finite volume method is to iterate the cell averages at every time step, starting with

$$u_j^0 = \frac{1}{\Delta x} \int_{x_{j-1/2}}^{x_{j+1/2}} u_0(x) dx$$

Now, let's suppose that we know the cell averages at a certain time level. How do we find the cell averages at the next time level ? If we integrate (2.1) over the spatial cell $[x_{j+1/2}, x_{j-1/2})$ and time interval $[t^n, t^{n+1})$,

$$\int_{t^n}^{t^{n+1}} \int_{x_{j-1/2}}^{x_{j+1/2}} u_t \; dxdt + \int_{t^n}^{t^{n+1}} \int_{x_{j-1/2}}^{x_{j+1/2}} f(u)_x \; dxdt = 0$$

hence,

$$\int_{x_{j-1/2}}^{x_{j+1/2}} u(x, t^{n+1}) \, dx - \int_{x_{j-1/2}}^{x_{j+1/2}} u(x, t^n) \, dx = - \int_{t^n}^{t^{n+1}} f(u(x_{j+1/2}, t) \, dt + \int_{t^n}^{t^{n+1}} f(u(x_{j-1/2}, t) \, dt$$

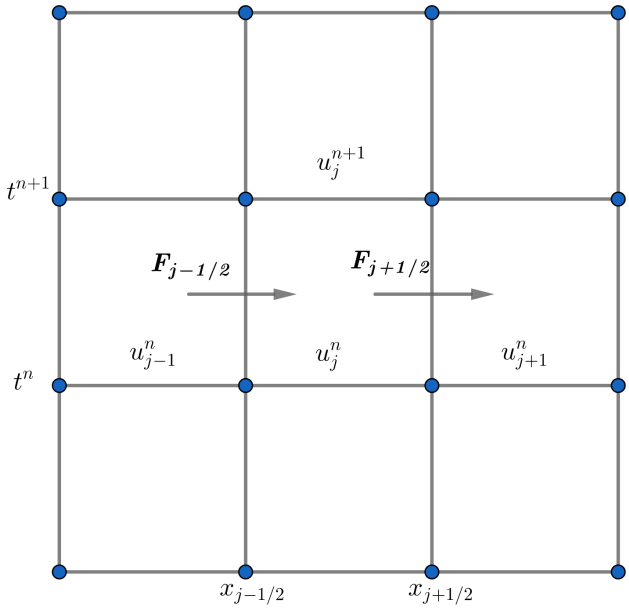

Figure 2.1: Finite volume grid displaying cell averages and fluxes

Defining

$$\bar{F}_{j+1/2}^n = \frac{1}{\Delta t} \int_{t^n}^{t^{n+1}} f(u(x_{j+1/2}, t)dt \tag{2.5}$$

and dividing both sides by Δx, it is obtained [5]

$$u_j^{n+1} = u_j^n - \frac{\Delta t}{\Delta x}(\bar{F}_{j+1/2}^n - \bar{F}_{j-1/2}^n) \tag{2.6}$$

It can be interpreted that the change of cell average is given by the difference in fluxes across the boundary of the cell. The main objective in a finite volume scheme is an efficient procedure to approximate fluxes $\bar{F}_{j-1/2}^n$, $\bar{F}_{j+1/2}^n$. We can see the illustration of the grid with cell averages and fluxes in the Figure 2.1.

Godunov came up with a brilliant approach for approximating the numerical fluxes in (2.6). As the cell averages u_j^n are constant in each spatial cell at each time level, Godunov figured that they define a Riemann problemn at each cell interface $x_{j+1/2}$ [12]:

$$\begin{cases} u_t + f(u)_x = 0 \\ u(x,t^n) = \begin{cases} u_j^n \ , \ if \ x < x_{j+1/2} \\ u_{j+1}^n \ , \ if \ x > x_{j+1/2} \end{cases} \end{cases} \tag{2.7}$$

Thus, at every time level, the cell averages define a superposition of Riemann problems of this form. The solution of each Riemann problem $\bar{u}_j(x,t)$ of (2.7) can be written as a function of a single variable $a = \frac{x-x_{j+1/2}}{t-t^n}$

$$\bar{u}_j(x,t) = \bar{u}_j(\frac{x - x_{j+1/2}}{t - t^n}) \tag{2.8}$$

Assuming the the continuity of the flux, it is observed that at $a = 0$, $f(\bar{u}_j(0))$ is well defined and $f(\bar{u}_j(0^+)) = f(\bar{u}_j(0^-))$. The edge-centered flux value can be defined as [5]

$$F_{j+1/2}^n := f(\bar{u}_j(0^+)) = f(\bar{u}_j(0^-))$$

The numerical flux does not change over the time hence can be explicitly computed as

$$\bar{F}_{j+1/2}^n = \frac{1}{\Delta t}\int_{t^n}^{t^{n+1}} f(u(x_{j+1/2},t) \ dt = F_{j+1/2}^n$$

If we plug that into (2.6),

$$u_j^{n+1} = u_j^n - \frac{\Delta t}{\Delta x}\big(F_{j+1/2}^n - F_{j-1/2}^n\big) \tag{2.9}$$

which is *the standard form of a finite volume scheme for conservation laws.*

We can compute explicit formulas for the numerical fluxes attaining the value of the flux of the Riemann problem at the interface $x_{j+1/2}$. Some different schemes to calculate numerical fluxes can be presented as follows.

2.2.2 Godunov Scheme

For non-convex flux functions, Godunov came up with the following formula to compute numerical flux [12]

$$F^n_{j+1/2} = F(u^n_j, u^n_{j+1}) = \begin{cases} \min_{u^n_j \le \theta \le u^n_{j+1}} \ f(\theta) \ if \ u^n_j \le u^n_{j+1} \\ \min_{u^n_{j+1} \le \theta \le u^n_j} \ f(\theta) \ if \ u^n_{j+1} \le u^n_j \end{cases}$$

This formula requires calculating an optimization problem, hence the computation can be complicated. Instead, we will benefit from the following fact to implement Godunov scheme.

Lemma 2.1. *If the flux function is strictly convex and f has a single minimum point at k and no local maxima, Godunov scheme can be rearranged as [5]*

$$F^n_{j+1/2} = F(u^n_j, u^n_{j+1}) = \max\left(f(\max(u^n_j, k)), f(\min(u^n_{j+1}, k))\right) \tag{2.10}$$

I will mainly be doing simulations for the solutions of Burger's equation. The flux function $\frac{u^2}{2}$, so there is a single minimum at 0. (2.10) can be rewritten for Burger's equation

$$F^n_{j+1/2} = F(u^n_j, u^n_{j+1}) = \max\left(f(\max(u^n_j, 0)), f(\min(u^n_{j+1}, 0))\right) \tag{2.11}$$

In the following numerical examples, the numerical flux (2.11) is used.

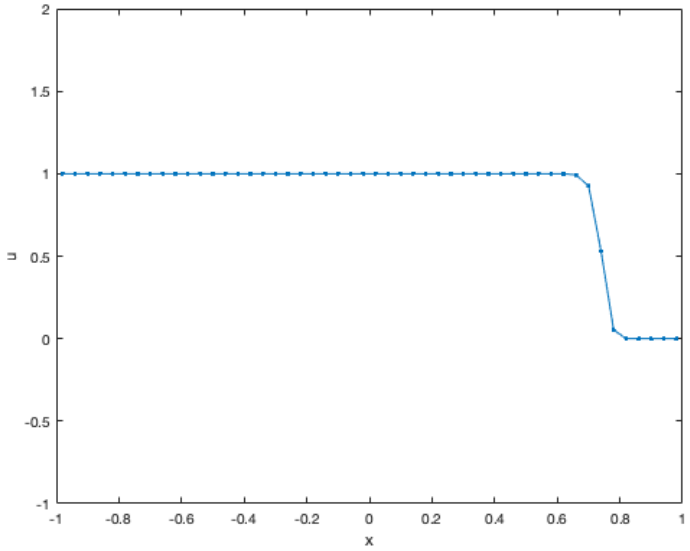

Figure 2.2: Godunov method applied to Example 2.1 at time t=1.5

Example 2.1. Consider Burger's equation (2.3) with the following Riemann data

$$u(x,0) = \begin{cases} 1 \; if \; x < 0 \\ 0 \; if \; x > 0 \end{cases}$$

The numerical solution with the spatial step size $h = 0.04$ can be seen in Figure 2.2. The solution doesn't oscillate nearby the shock and is stable.

Example 2.2. Consider another Burger's equation (2.3) with the initial data

$$u(x,0) = \sin(4\pi x) \;\; -1 \leq x \leq 1$$

Using periodic boundary conditions and with the step size $h = 0.04$, the numerical solution obtained by Godunov scheme is plotted in Figure (2.3). The solution includes both shocks and rarefaction waves which is why it is called *N-wave*.

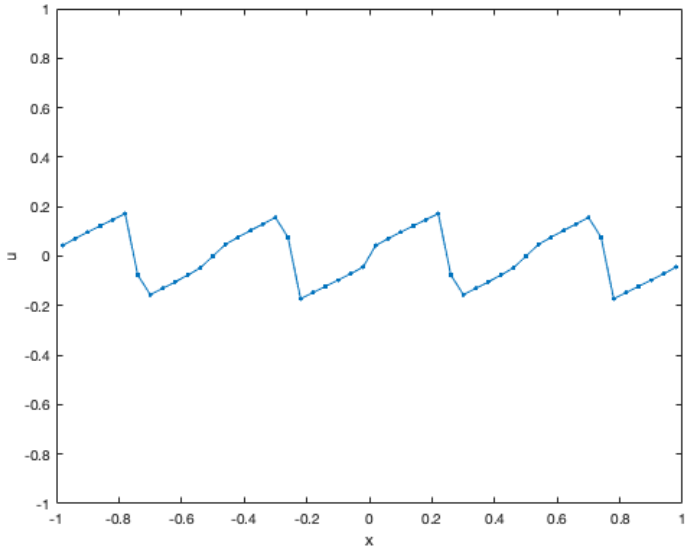

Figure 2.3: Godunov method applied to Example 2.2 at time t=1.5

Next, we will see some approaches that approximate the solutions of the Riemann problem by replacing the exact solution with two waves, one traveling to the left of the interface with speed $s^l_{j+1/2}$, and another to the right $s^r_{j+1/2}$ [5].

Lemma 2.2. *(Rankine-Hugoniot condition) The classical paradigm about PDEs is that the solutions must be differentiable functions. However, the weak solutions have to be neither differentiable nor continuous. This implies that weak solutions can contain discontinuities. These discontinuities appear in nature as shock waves. The shock speed must satisfy [5]*

$$s(t) = \frac{f(u_R(t)) - f(u_L(t))}{u_R(t) - u_L(t)} \tag{2.12}$$

Now, let's consider the approximation to the solution of (2.7)

$$u(x,t) = \begin{cases} u^n_j \quad if \quad x < s^l_{j+1/2}t \\ u^n_{j+1/2} \quad if \quad s^l_{j+1/2}t < x < s^r_{j+1/2}t \\ u^n_{j+1} \quad if \quad x > s^r_{j+1/2}t \end{cases} \tag{2.13}$$

applying Rankine-Hugoniot condition

$$\begin{cases} f(u^n_{j+1}) - f^n_{j+1/2} = s^r_{j+1/2}(u^n_{j+1} - u^n_{j+1/2}) \\ f(u^n_j) - f^n_{j+1/2} = s^l_{j+1/2}(u^n_j - u^n_{j+1/2}) \end{cases}$$

If we solve this system for $f^n_{j+1/2}$

$$f^n_{j+1/2} = \frac{s^r_{j+1/2} f(u^n_j) - s^l_{j+1/2} f(u^n_{j+1}) + s^r_{j+1/2} s^l_{j+1/2}(u^n_{j+1} - u^n_j)}{s^r_{j+1/2} - s^l_{j+1/2}} \tag{2.14}$$

and choose the wave speeds to be equal in opposite signs, $s^r_{j+1/2} = -s^l_{j+1/2} = s$. (2.14) simplifies to

$$f^n_{j+1/2} = \frac{f(u^n_{j+1}) + f(u^n_j)}{2} - \frac{s(u^n_{j+1} - u^n_j)}{2} \tag{2.15}$$

Different choices of the speeds will describe different schemes. Three of them are presented as follows [5].

2.2.3 Lax-Friedrichs Scheme

To ensure that waves occurring at neighboring Riemann problems not to interact 2.13, Lax-Friedrichs have chosen the wave speeds as [5]

$$s^r_{j+1/2} = -\frac{\Delta x}{\Delta t} \ , s^r_{j+1/2} = \frac{\Delta x}{\Delta t}$$

If we plug these into (2.15) we get Lax-Friedrichs flux

$$F^n_{j+1/2} = \frac{f(u^n_{j+1}) + f(u^n_j)}{2} - \frac{\Delta t}{2\Delta x}(u^n_{j+1} - u^n_j) \tag{2.16}$$

to be substituted into (2.9).

The numerical results for Example 2.2 using Lax-Friedrichs scheme is plotted in Figure (2.4). We can observe the obvious diffusions nearby the shock.

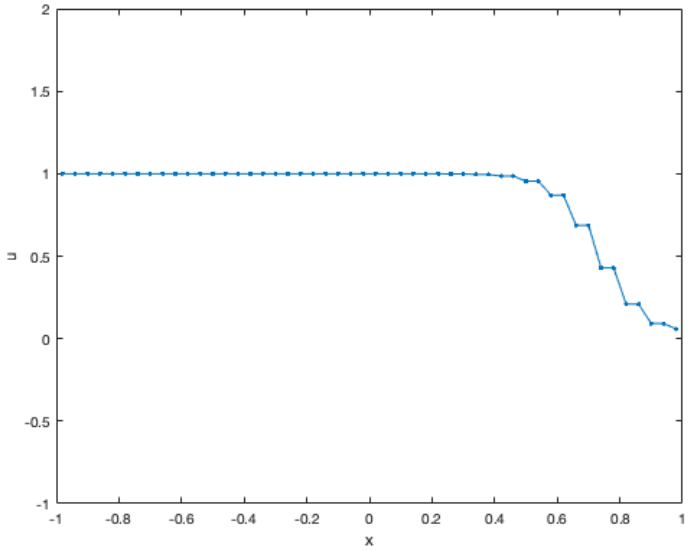

Figure 2.4: Lax Friedrichs method applied to Example 2.1 at t=1.5

2.2.4 Rusanov Scheme

The Lax Friedrichs scheme is very diffusive around shocks. The main reason for that lies in the choice of the wave speeds. These speeds were the maximum allowed speeds and did not take into the account the speeds of propagation of the problem under consideration. An improvement in the choice of speeds can be made by locally selecting [5]

$$s^r_{j+1/2} = -s^l_{j+1/2} = \max(|f'(u^n_j)|, |f'(u^n_{j+1})|)$$

If we plug this into (2.15)

$$F^n_{j+1/2} = \frac{f(u^n_{j+1}) + f(u^n_j)}{2} - \frac{\max(|f'(u^n_j)|, |f'(u^n_{j+1})|)}{2}(u^n_{j+1} - u^n_j)$$

Example 2.3. Consider Burger's equation (2.3) with the following Riemann data

$$u(x,0) = \begin{cases} 1 \ if \ x < 0 \\ -1 \ if \ x > 0 \end{cases}$$

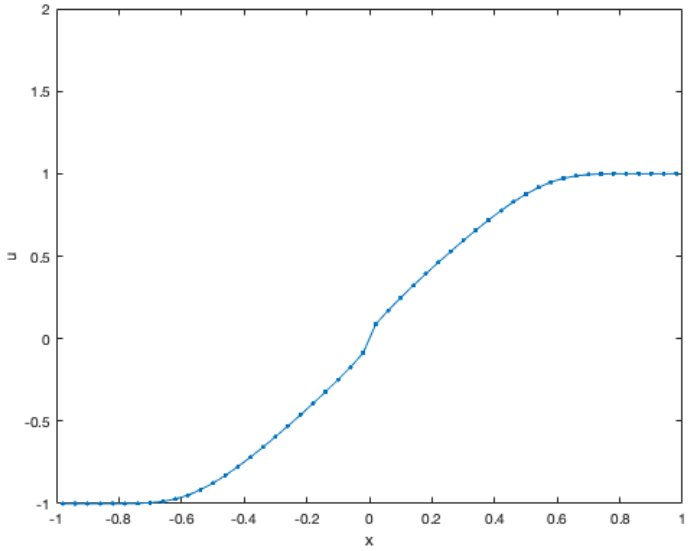

Figure 2.5: Rusanov method applied to Example 2.3 at t=0.5

Figure (2.5) shows the numerical result which is the rarefaction wave solution.

2.2.5 Engquist-Osher Scheme

Engquist-Osher scheme has the flux [5]

$$F^n_{j+1/2} = \frac{f(u^n_{j+1}) + f(u^n_j)}{2} - \frac{1}{2}\int_{u^n_j}^{u^n_{j+1}} |f'(x)|dx$$

When f has a single minimum k and no maxima, i.e. Burger's equation, Engquist-Osher flux can be rearranged as

$$F^n_{j+1/2} = f(\max(u^n_j, k)) + f(\min(u^n_{j+1}, k)) - f(k)$$

When we plug the flux into (2.9) the term $f(k)$ will get cancelled. Hence, we can rewrite the flux

$$F^n_{j+1/2} = f(\max(u^n_j, k)) + f(\min(u^n_{j+1}, k))$$

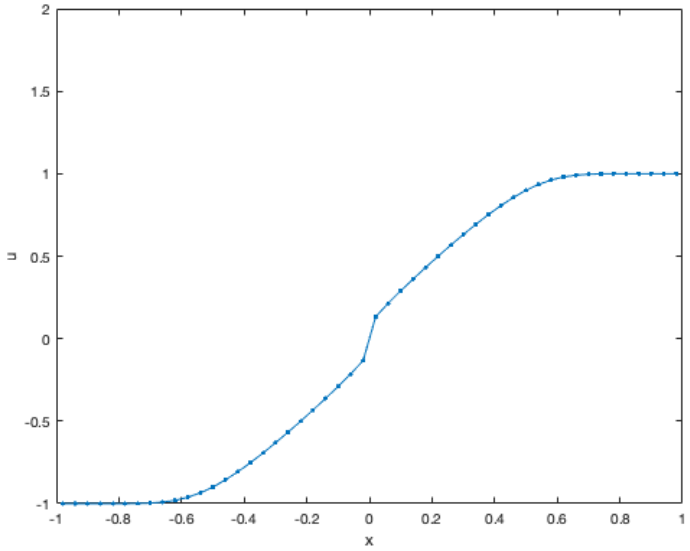

Figure 2.6: Engquist-Osher method applied to Example 2.2 at t=0.5

Therefore, Engquist Osher scheme is regarded as flux splitting scheme which splits the flux into its negative and positive parts taking the direction of propagation into account. In the particular case Burger's equation, it should be recalled that $k = 0$.

The numerical solution of Example 2.2 with Engquist-Osher flux can be seen in Figure 2.6. Like Rusanov scheme, we can see the rarefaction wave formation without lots of diffusions.

- Comparison of Finite Volume Schemes

We compare all the numerical fuxes presented in this section for two sets of initial data. In other words, the behaviour of each scheme for shock wave and rarefaction wave solutions. First, we consider Example 2.1 and compare the four different numerical fluxes we've used on a mesh consisting of 50 points. We can see the shock wave formation and how each scheme handles the shock in Figure 2.7. It reveals that Godunov and Engquist-Osher are superior to Rusanov and Lax Friedrichs in terms of the behaviour and stability nearby the shock wave.

Secondly, the comparison of finite volume schemes for Example 2.2 is shown in Figure 2.8. The solution involves rarefaction wave because of the initial data. Again, Godinov

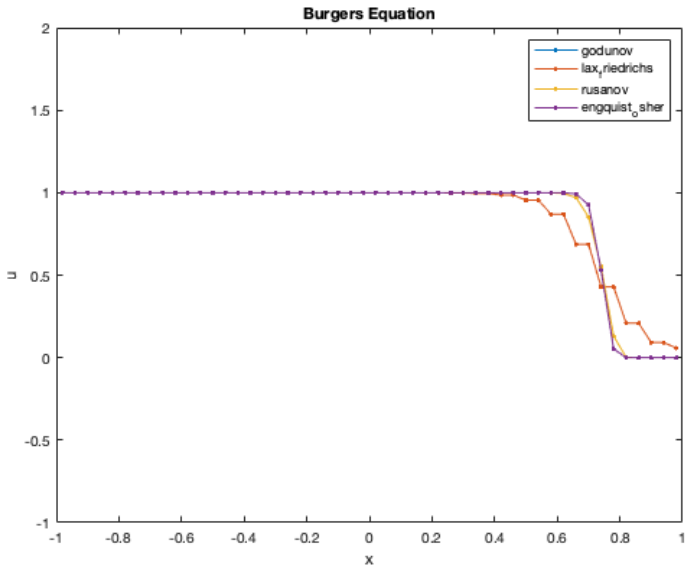

Figure 2.7: Comparison of all methods for Example 2.1 at t=0.5

and Engquist-Osher have turned out to be most efficient schemes in terms of capturing the rarefaction waves.

It should be noted that in both cases Lax-Friedrichs and Rusanov schemes have faster run times than other two methods. However, since our aim is to obtain efficiency nearby the shock and rarefaction waves, we will use Godunov and Engquist Osher schemes when we do simulations for Random Conservation Laws.

2.3 Flux Limiter Methods

High order flux methods like Lax-Wendroff scheme do not behave well at discontinuities and low order flux methods like the upwind scheme do not work well in smooth regions. To benefit from the advantages of both types of methods, *high resolution methods*, which are at least second order accurate on smooth solutions and reduce the amount of numerical dissipation nearby the discontinuities, have been studied to solve nonlinear conservation laws.

In particular, the flux limiter method with which we can arrange the flux depending on the region can be useful. One can rewrite high order flux as the sum of low order flux and corrector [6]

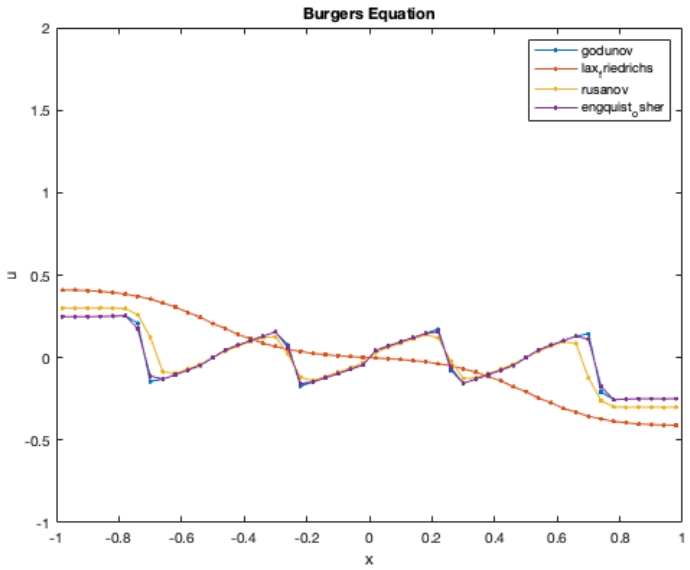

Figure 2.8: Comparison of all methods for Example 2.2 at t=0.5

$$f_H = f_L + [f_H - f_L].$$

In a flux limiter method, the magnitude of this correction depends on the data, so the flux becomses

$$f_H = f_L + \phi[f_H - f_L],$$

where ϕ is the limiter. ϕ is chosen as near 1 if data is smooth and we want it to be close to 0 near discontinuities. One particular flux limiter method which have been presented by Galiano and Zapata as follows

- TVD Flux Limiter Method [4]

Consider the conservative hyperbolic equation

$$\begin{cases} u_t + f(u)_x = 0, \ x \in \mathbb{R} \ t \geq 0 \\ u(x,0) = u_0(x) \end{cases}$$

where $u = u(x,t)$ is a scalar field carried along by a nonlinear flux function $f = f(x,t)$.

Definition 2.1. A numerical method is called *Total Variation Diminishing (TVD)* if for all grid functions u^n,

$$TV(U^{n+1}) \leq TV(U^n)$$

where

$$TV(U^n) = \sum_j |u^n_{j+1} - u^n_j|$$

The aim of the new method is to build a method that reduces the numerical diffusion at discontinuities and is accurate and TVD stable. In order to do that, second order accurate in smooth regions Richtmyer two-step Lax Wendroff method will be incorporated in first order accurate in shock wave solutions conservative upwind scheme .

Defining the discrete mesh points (x_j, t_n) by $x_j = jh$ and $t_n = nk$ where $j \in \mathbb{Z}$ and $n \in \mathbb{N}$, h is the spatial size and k is the time step. The Richtmyer two-step Lax Wendroff scheme has the predictors

$$u^{n+1/2}_{j+1/2} = \frac{1}{2}\big[u^n_{j+1} + u^n_j - \frac{k}{h}(f(u^n_{j+1}) - f(u^n_j))\big] \tag{2.17}$$

$$u^{n+1/2}_{j-1/2} = \frac{1}{2}\big[u^n_j + u^n_{j-1} - \frac{k}{h}(f(u^n_j) - f(u^n_{j-1}))\big] \tag{2.18}$$

with the corrector step

$$u^{n+1}_j = u^n_j = \frac{k}{h}\big[f(u^{n+1/2}_{j+1/2}) - f(u^{n+1/2}_{j-1/2})\big]$$

The upwind scheme is given by

$$u^{n+1}_j = u^n_j - \frac{k}{h}\big[\lambda^+(f(u^n_j) - f(u^n_{j-1})) - \lambda^-(f(u^n_{j+1}) - f(u^n_j))\big]$$

where

$$\lambda^+ = \max\Big(\frac{f_u(u_j^n)}{|f_u(u_j^n)|}, 0\Big),\ \lambda^- = \min\Big(\frac{f_u(u_j^n)}{|f_u(u_j^n)|}, 0\Big)$$

If we add the new approximation point $u_j^{n+1/2}$ in the predictor step of Richtmyer two-step Lax Wendroff method using upwind scheme,

$$u_j^{n+1/2} = u_j^n - \frac{k}{2h}\big[\lambda^+(f(u_j^n) - f(u_{j-1}^n)) - \lambda^-(f(u_{j+1}^n) - f(u_j^n))\big] \tag{2.19}$$

We can write the corrector step of flux limiter scheme proposed by Galiano and Zapata with the predictors (2.17), (2.18) and (2.19),

$$u_j^{n+1} = u_j^{n+1/2} - \frac{k}{h}\Big[\phi(\theta_j^{n+1/2})\big(f(u_{j+1/2}^{n+1/2}) - f(u_j^{n+1/2})\big) - \phi(\theta_{j-1/2}^{n+1/2})\big(f(u_j^{n+1/2}) - f(u_{j-1/2}^{n+1/2})\big)\Big]$$

where

$$\theta_j^{n+1/2} = \frac{|f(u_j^{n+1/2}) - f(u_{j-1/2}^{n+1/2})|}{|f(u_{j+1/2}^{n+1/2}) - f(u_j^{n+1/2})| + |f(u_j^{n+1/2}) - f(u_{j-1/2}^{n+1/2})|}$$

$$\theta_{j-1/2}^{n+1/2} = 1 - \theta_j^{n+1/2}$$

The flux function ϕ is defined as

$$\phi(\theta_j^{n+1/2}) = \begin{cases} 0 \quad b_j^n \le 0, \\ \begin{cases} \theta_j^{n+1/2} & b_j^n > 0 \ and \ |\frac{k}{h} f_u(u_j^n)| \le \frac{1}{2} \\ \frac{1}{2}\theta_j^{n+1/2} & b_j^n > 0 \ and \ |\frac{k}{h} f_u(u_j^n)| > \frac{1}{2} \end{cases} \end{cases}$$

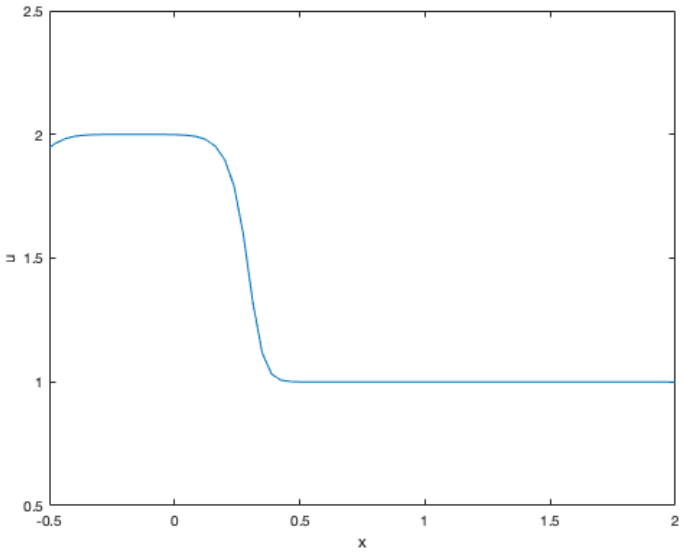

Figure 2.9: Flux limiter method applied to Example 2.4 at t=0.4

with the local flow parameter

$$b_j^n = \begin{cases} \frac{u_{j+1}^n - u_j^n}{u_j^n - u_{j+1}^n} & \frac{k}{h} f_u(u_j^n) \geq 0 \\ \frac{u_j^n - u_{j-1}^n}{u_{j+1}^n - u_j^n} & \frac{k}{h} f_u(u_j^n) < 0 \end{cases}$$

Example 2.4. Consider Burger's equation (2.3) with the following Riemann data

$$u(x,0) = \begin{cases} 2 \; if \; x < 0 \\ 1 \; if \; x > 0 \end{cases}$$

The numerical result with the spatial step size $h = 0.0125$ is shown in Figure (2.9). The solution does not disperse nearby the shock and is stable.

Some numerical properties of the methods such as consistency, linear stability and TVD stability have been shown by Galiano and Zapata [4]. I will give details on proving the consistency.

Proposition 2.1. *The scheme is consistent. In fact, it is first order accurate in time and second or first order accurate in space depending on the value of θ.*

Proof: It needs to be shown that truncation error

$$\Gamma_j^n(u) = L_{h,k}u_j^n - Lu = L_{h,k}u_j^n - (u_t + f(u)_x)$$

goes to zero as $h, k \to 0$. Assuming u and $f(u)$ are smooth functions, we can use Taylor expansions about (x, t).

$$L_{h,k}u_j^n = u_j^{n+1} - u_j^{n+1/2} + \frac{k}{h}\Big[\theta\big(f(u_{j+1/2}^{n+1/2}) - f(u_j^{n+1/2})\big) + (1-\theta)\big(f(u_j^{n+1/2}) - f(u_{j-1/2}^{n+1/2})\big)\Big]$$

with

$$u_j^{n+1} = u(x_j, t_{n+1/2}) + \frac{k}{2}u_t(x_j, t_{n+1/2}) + k^2\frac{u_{tt}(x_j, t_{n+1/2})}{8} + k^3\frac{u_{ttt}(x_j, t_{n+1/2})}{48} + O(k^4)$$

and

$$f(u_{j\pm1/2}^{n+1/2}) = f(u(x_j, t_{n+1/2})) \pm \frac{h}{2}f(u(x_j, t_{n+1/2})_x + h^2\frac{f(u(x_j, t_{n+1/2}))_{xx}}{8} \pm h^3\frac{f(u(x_j, t_{n+1/2}))_{xxx}}{48} + O(h^4)$$

hence

$$\begin{aligned}\Gamma_j^n(u) &= L_{h,k}u_j^n - Lu \\ &= \frac{k}{2}u_t + \frac{k^2}{8}u_{tt} + \frac{k^3}{8}u_{ttt} + O(k^4) + \frac{k}{h}\Big[\theta\big(\frac{h}{2}f(u)_x + \frac{h^2}{8}f(u)_{xx} + \frac{h^3}{48}f(u)_{xxx} + O(h^4)\big) \\ &\qquad + (1-\theta)\big(\frac{h}{2}f(u)_x - \frac{h^2}{8}f(u)_{xx} + \frac{h^3}{48}f(u)_{xxx} - O(h^4)\big)\Big] - u_t - f(u)_x \quad (2.20)\end{aligned}$$

If we benefit from

$$u_t = -f(u)_x \Rightarrow u_{tt} = -f(u)_{xt} \Rightarrow u_{ttt} = -f(u)_{xtt}$$

The truncation error simplifies to

$$-\frac{k}{8}f(u)_{xt} - \frac{k^2}{48}f(u)_{xtt} + O(k^3) + +(2\theta-1)\frac{h}{8}f(u)_{xx} + \frac{h^2}{48}f(u)_{xxx} + (2\theta-1)O(h^3)$$

thus

$$\Gamma_j^n(u) = (2\theta-1)O(h) + O(h^2) + O(k^2)$$

It should be noted that if the solution is in the smooth region, θ is expected to be close to $1/2$ so the scheme would be second order accurate in space.

Proposition 2.2. *The scheme is TVD stable if the CFL condition is satisfied:*

$$\left|\frac{k}{h}f_u(u_j^n)\right| \leq 1 \quad \forall j, n$$

2.4 Conservation Laws in Heterogeneous Media

If the flux function is spatially dependent (heterogeneous), system (2.1) can be rewritten as:

$$u_t + f(u,x)_x = 0 \tag{2.21}$$

where $u(x,t) \in \mathbb{R}^m$ and $f : \mathbb{R}^m \times \mathbb{R} \to \mathbb{R}^m$.

Let's reconsider Riemann problem with initial data at each cell interface $x_{j-1/2}$:

$$u(x,0) = \begin{cases} U_{j-1} & if\ x < x_{j-1/2} \\ U_j & if\ x > x_{j-1/2} \end{cases} \tag{2.22}$$

Riemann solution of m equations is m waves that are denoted by $W^p_{i-1/2}$ propagating with speeds $s_{j-1/2}$ where $p = 1, 2, ..., m$ and $m = 1$ is the scalar case[24].

We have previously seen that Riemann solution involves discontinous waves (shocks) and initial difference can be decomposed

$$U_j - U_{j-1} = \sum_{p=1}^{m} W^p_{j-1/2} \tag{2.23}$$

Using the finite volume and cell average approach covered in this chapter, the flux function $f(u, x)$ can be discretized using cell centered flux function. In other words, the flux function is assumed to take the same value throughout the ith cell. Hence, (2.21) can be rewritten as Riemann problem at each interface as follows [24]

$$u_t + F_{j-1/2}(u, x)_x = 0$$

where

$$F_{j-1/2}(u, x) = \begin{cases} f_{j-1}(u) & if\ x < x_{j-1/2} \\ f_j(u) & if\ x > x_{j-1/2} \end{cases}$$

Bae, Leveque, Mitran and Rosmanith [24] decomposed flux difference between cells into waves and used that in wave propagation algorithm to solve (2.21). The algorithm is based on eigenvalues $s^p_{j-1/2}$ and eigenvectors $r^p_{j-1/2}$ of approximate Jacobian matrix $A_{j-1/2}$ which will be computed using $f(U_{j-1})$ and $f(U_j)$ for $p = 1, 2, ..., m$. The flux difference can be decomposed as a linear combination of the eigenvectors

$$f_j(U_j) - f_{j-1}(U_{j-1}) = \sum_{p=1}^{m} \beta^p_{j-1/2} r^p_{j-1/2} = \sum_{p=1}^{m} Z^p_{j-1/2}$$

with

$$\beta_{j-1/2} = R^{-1}_{j-1/2}(f_j(U_j) - f_{j-1}(U_{j-1}))$$

The vectors $Z^p_{j-1/2}$ are called *f-waves*. The Riemann solution (2.23) can also be written as a linear combination of eigenvectors

$$U_j - U_{j-1} = \sum_{p=1}^{m} W^p_{j-1/2} = \sum_{p=1}^{m} \alpha^p_{j-1/2} r^p_{j-1/2} \tag{2.24}$$

One of the famous approaches to approximate Jacobian matrix $A_{j-1/2}$ is *Roe average*:

$$A_{j-1/2}(U_j - U_{j-1}) = f_j(U_j) - f_{j-1}(U_{j-1}) \tag{2.25}$$

Multiplying both sides of (2.24) by $A_{j-1/2}$ and using the fact $s^p_{j-1/2}$ is eigenvalue of $A_{j-1/2}$

$$f_j(U_j) - f_{j-1}(U_{j-1}) = \sum_{p=1}^{m} \alpha^p_{j-1/2} s^p_{j-1/2} r^p_{j-1/2} = \sum_{p=1}^{m} Z^p_{j-1/2} \tag{2.26}$$

and it follows from (2.24) and (2.26) that $Z^p_{j-1/2} = s^p_{j-1/2} W^p_{j-1/2}$.

The wave propagation algorithm [24] can be obtained as follows

$$U^{n+1}_j = U^n_j - \frac{\Delta t}{\Delta x}\Big[\sum_{p=1}^{m} (s^p_{j-1/2})^+ W^p_{j-1/2} + \sum_{p=1}^{m} (s^p_{j-1/2})^- W^p_{j-1/2}\Big]$$

where $s^+ = \max(s, 0)$ and $s^- = \min(s, 0)$. We should notice that this is how fluctuations are seperated as right going waves $s > 0$ and left going waves $s < 0$. To upgrade this algorithm to a high resolution method, correction fluxes can be added

$$U^{n+1}_j = U^n_j - \frac{\Delta t}{\Delta x}\Big[\sum_{p=1}^{m} (s^p_{j-1/2})^+ W^p_{j-1/2} + \sum_{p=1}^{m} (s^p_{j-1/2})^- W^p_{j-1/2}\Big] - \frac{\Delta t}{\Delta x}[\tilde{F}_{j+1/2} - \tilde{F}_{j-1/2}] \tag{2.27}$$

where

$$\tilde{F}_{j+1/2} = \frac{1}{2}\sum_{p=1}^{m} |s^p_{j+1/2}|\Big(1 - \frac{\Delta t}{\Delta x}|s^p_{j+1/2}|\Big)\tilde{W}^p_{j+1/2} \tag{2.28}$$

Here $\tilde{W}_{j+1/2}$ is the limited version of $W_{j+1/2}$, obtained by comparing $W_{j+1/2}$ to $W_{K+1/2}$ which is the wave from the adjacent Riemann problem on the upwind side,

$$K = \begin{cases} j-1 & if \quad s^p_{j+1/2} > 0 \\ j+1 & if \quad s^p_{j+1/2} < 0 \end{cases}$$

Using the fact that $\tilde{Z}^p_{j+1/2} = s^p_{j+1/2}\tilde{W}^p_{j+1/2}$, (2.27) can be rearranged as

$$\tilde{F}_{j+1/2} = \frac{1}{2}\sum_{p=1}^{m} sgn(s^p_{j+1/2})\Big(1 - \frac{\Delta t}{\Delta x}|s^p_{j+1/2}|\Big)\tilde{Z}^p_{j+1/2}$$

And wave propagation algorithm (2.27) can be rewritten as

$$\begin{aligned} U^{n+1}_j = U^n_j &- \frac{\Delta t}{\Delta x}\Bigg[\sum_{p:s^p_{j-1/2}>0} Z^p_{j-1/2} + \sum_{p:s^p_{j+1/2}<0} Z^p_{j+1/2}\Bigg] \\ &- \frac{\Delta t}{2\Delta x}\Bigg[\sum_{p=1}^{m} sgn(s^p_{j+1/2})\Big(1 - \frac{\Delta t}{\Delta x}|s^p_{j+1/2}|\Big)Z^p_{j+1/2} - \sum_{p=1}^{m} sgn(s^p_{j-1/2})\Big(1 - \frac{\Delta t}{\Delta x}|s^p_{j-1/2}|\Big)Z^p_{j-1/2}\Bigg] \end{aligned}$$

Without loss of generality, let's assume $p : s^p_{j+1/2} > 0$ is satisfied for $p = 1, .., k$ and $p : s^p_{j-1/2} > 0$ is satisfied for $p = 1, .., t$. Then this expression can be simplified as

$$\begin{aligned} U^{n+1}_j = U^n_j &- \frac{\Delta t}{\Delta x}\Big[\sum_{p=1}^{t} Z^p_{j-1/2} + \sum_{p=k+1}^{m} Z^p_{j+1/2}\Big] \\ &- \frac{\Delta t}{2\Delta x}\Big[-\sum_{p=k+1}^{m} Z^p_{j+1/2}(1 + \frac{\Delta t}{\Delta x}s^p_{j+1/2}) + \sum_{p=t+1}^{m} Z^p_{j-1/2}(1 + \frac{\Delta t}{\Delta x}s^p_{j-1/2})\Big] \\ &- \frac{\Delta t}{2\Delta x}\Big[\sum_{p=1}^{k} Z^p_{j+1/2}(1 - \frac{\Delta t}{\Delta x}s^p_{j+1/2}) - \sum_{p=1}^{t} Z^p_{j-1/2}(1 - \frac{\Delta t}{\Delta x}s^p_{j-1/2})\Big] \end{aligned}$$

and then

$$U_j^{n+1} = U_j^n - \frac{\Delta t}{2\Delta x}\Big[2\sum_{p=1}^{t} Z_{j-1/2}^p + \sum_{p=t+1}^{m} Z_{j-1/2}^p - \sum_{p=1}^{t} Z_{j-1/2}^p$$
$$2\sum_{p=k+1}^{m} Z_{j+1/2}^p + \sum_{p=1}^{k} Z_{j+1/2}^p - \sum_{p=k+1}^{m} Z_{j+1/2}^p\Big]$$
$$+ \frac{\Delta t^2}{2\Delta x^2}\Big[\sum_{p=k+1}^{m} Z_{j+1/2}^p s_{j+1/2}^p - \sum_{p=t+1}^{m} Z_{j-1/2}^p s_{j-1/2}^p + \sum_{p=1}^{k} Z_{j+1/2}^p s_{j+1/2}^p - \sum_{p=1}^{t} Z_{j-1/2}^p s_{j-1/2}^p\Big]$$

Hence, the finalized version of wave propagation algorithm is

$$U_j^{n+1} = U_j^n - \frac{\Delta t}{2\Delta x}\Big[\sum_{p=1}^{m}\big(Z_{j-1/2}^p + Z_{j+1/2}^p\big)\Big] + \frac{\Delta t^2}{2\Delta x^2}\Big[\sum_{p=1}^{m}\big(Z_{j+1/2}^p s_{j+1/2}^p - Z_{j-1/2}^p s_{j-1/2}^p\big)\Big]$$

Now we can show the method is second order accurate [24]. Recalling that $s_p^{j+1/2}$ is eigenvalue of A we can get,

$$U_j^{n+1} = U_j^n - \frac{\Delta t}{2\Delta x}\Big[\sum_{p=1}^{m}\big(Z_{j-1/2}^p + Z_{j+1/2}^p\big)\Big] + \frac{\Delta t^2}{2\Delta x^2}\Big[A_{j+1/2}\sum_{p=1}^{m} Z_{j+1/2}^p - A_{j-1/2}\sum_{p=1}^{m} Z_{j-1/2}^p\Big] \tag{2.29}$$

Provided that the flux $f(u,x)$ is smooth in x, we rewrite *f-waves*

$$f(U_j, x_j) - f(U_{j-1}, x_{j-1}) = \sum_{p=1}^{m} Z_{j-1/2}^p \tag{2.30}$$

and plug that into (2.29)

$$U_j^{n+1} = U_j^n - \frac{\Delta t}{2\Delta x}(f(U_{j+1}, x_{j+1}) - f(U_{j-1}, x_{j-1})) + \frac{\Delta t^2}{2\Delta x^2}[A_{j+1/2}(f(U_{j+1}, x_{j+1}) - f(U_j, x_j)) - A_{j-1/2}(f(U_j, x_j) - f(U_{j-1}, x_{j-1}))]$$

this matches with the Taylor series expansion of the exact solution. We know from (2.21) that $u_t + f(u,x)_x = 0$, therefore

$$u_t = -f(u,x)_x$$
$$u_{tt} = -[f(u,x)_x]_t = [f(u,x)_t]_x = -[f_u(u,x)u_t]_x = [f_u(u,x)f(u,x)_x]_x$$

taking $A_{j-1/2} = f'_{j-1}(U_{j-1})$ and $A_{j+1/2} = f'_j(U_j)$, we obtain

$$u(x, t_{n+1}) = u(x, t^n) - \Delta t f(u,x)_x + \frac{1}{2}\Delta t^2 [f_u(u,x)f(u,x)_x]_x + \mathcal{O}(\Delta t^3)$$
$$\Rightarrow u(x_j, t_{n+1}) = u(x_j, t^n) + \Delta t u_t(x_j, t^n) + \frac{1}{2}\Delta t^2 u_{tt}(x_j, t^n) + \mathcal{O}(\Delta t^3)$$

and $\mathcal{O}(\Delta t^3)$ can be replaced by $\mathcal{O}(\Delta t \Delta x^2)$.

Chapter 3

Random Conservation Laws

Let's reconsider the system of conservation laws with random inputs:

$$\begin{cases} \partial_t U(x,t,\omega) + \nabla_x \cdot F(U,\omega) = 0 \\ U(x,0,\omega) = U_0(x,\omega) \end{cases} \tag{3.1}$$

To develop efficient algorithms for quantifying uncertainty in solutions of conservation laws with random inputs is difficult. One challenge is that discontinuities in the solution in physical space translates into the random solution. Another challenge is the curse of dimensionality which is as the dimension of space increases the available information becomes sparse and the uncertainty is getting very large, especially when parameter space is complex. Our mathematical formulation of scalar conservation laws with random data will use the concept of random variables taking values in function spaces. We will need some preliminary probability definitions.

3.1 Random Fields

Definition 3.1. A *probability space* is a triple $(\Omega, \mathcal{F}, \mathbb{P})$ where Ω is a sample space (set of outcomes); $\mathcal{F}$ is a collection of events that include Ω and $\varnothing$ with the property that $\mathcal{F}$ is closed under countable intersections and unions, complementation ; $\mathbb{P}$ is a probability function that assigns probability to events in $\mathcal{F}$,i.e. $\mathbb{P}(\Omega) = 1$ and $\mathbb{P}(\varnothing) = 0$ [8].

On Ω, any real-valued function X defined is a *random variable*. If (E, G) is a second measurable space, then an E-valued random variable is any mapping $X : \Omega \to E$ such that the set $\{\ \omega \in \Omega : X(\omega) \in A\} \in \mathcal{F}$ for any $A \in G$ meaning X is a G-measurable mapping from Ω into E [3].

Lemma 3.1. *With the assumption that E is a metric space and the Borel σ-field $\mathcal{B}(E)$; the set of all integrable, E-valued random variables X is denoted by $L^1(\Omega, \mathcal{F}, \mathbb{P}; E)$. It is equipped with the norm [3]*

$$||X||_{L^1(\Omega;E)} = \int_\Omega ||X(\omega)||_E \mathbb{P}(d\Omega) = \mathbb{E}(||X||_E)$$

More generally, for $1 \leq p \leq \infty$ $L^1(\Omega, \mathcal{F}, \mathbb{P}; E)$ is defined as the set of p-summable random variables taking values in E and is equipped with norm

$$||X||_{L^p(\Omega;E)} := (\mathbb{E}(||X||_E^p))^{1/p}, \quad 1 \leq p \leq \infty$$

Definition 3.2. A *random field* is a measurable mapping $U : \omega \mapsto U(x, t, \omega)$ from $(\Omega, \mathcal{F})$ to $((C([0, T], L^1(\mathbb{R}^d))^m \ , \mathcal{B}((C([0, T], L^1(\mathbb{R}^d)))^m)$.

To deal with uncertainty, let's suppose $(\Omega, \mathcal{F}, \mathbb{P})$ is the underlying probability space . The uncertain inital data can be modeled as a random field

$$U_0 : (\Omega, \mathcal{F}) \mapsto (L^1(\mathbb{R}^d)^m, \mathcal{B}((L^1(\mathbb{R}^d))^m)) \tag{3.2}$$

Similarly, the flux function can be modeled as random field

$$F : (\Omega, \mathcal{F}) \mapsto (C^1(\mathbb{R}; \mathbb{R}^d)^m, \mathcal{B}((C^1(\mathbb{R}; \mathbb{R}^d))^m))$$

Using these random fields, Mishra and Schwab defined the random entropy solution of U of (3.1) [13].

Definition 3.3. A random field $U : \Omega \mapsto (L^1_{loc}(\mathbb{R}^d \times \mathbb{R}_+))^m$ is a *random entropy solution* of the random conservation law (3.1) with random initial data, flux, if it satisfies the following two conditions for all test functions $\varphi \in C^1_0(\mathbb{R}^d \times \mathbb{R}_+)$:

1. *Weak Solution*: For almost every $\omega \in \Omega$, $U(.,.,\omega)$ satisfies the following integral identity, :

$$\int_{\mathbb{R}_+}\int_{\mathbb{R}^d}\left(U(x,t,\omega)\varphi_t(x,t)+\sum_{j=1}^{d}F^j(U(x,t,\omega),\omega)\frac{\partial}{\partial x_j}\varphi(x,t)\right)dxdt + \int_{\mathbb{R}^d}U_0(x,\omega)\varphi(x,0)dx=0$$

2. *Entropy Condition*: For any pair of deterministic entropy η and stochastic entropy flux $Q(\omega;\cdot)$ (i.e. η, Q_j with $j=1,2,...,d$ are functions such that η is convex and such that $Q'_j(\omega;\cdot)=\eta' F'_j(\omega;\cdot)$ for all j) and for almost every $\omega\in\Omega$, U satisfies the inequality

$$\int_{\mathbb{R}_+}\int_{\mathbb{R}^d}\left(\eta U(x,t,\omega)\varphi_t(x,t)+\sum_{j=1}^{d}Q^j(U(x,t,\omega),\omega)\frac{\partial}{\partial x_j}\varphi(x,t)\right)dxdt + \int_{\mathbb{R}^d}\eta U_0(x,\omega)\varphi(x,0)dx\geq 0$$

The random entropy solutions have been shown to be of the form [13]

$$U(x,t,\omega)=\mathcal{S}_t(U_0(x,\omega))$$

where $\mathcal{S}_t : L^p(D)\mapsto L^p(D)$ with $D\subset\mathbb{R}^d$ is the data to solution operator of the underlying deterministic problem. Rigorous existence and uniqueness results for random entropy solutions for scalar conservation laws, with random initial data, were obtained by Mishra and Schwab [13]. Well-posedness results for scalar conservation laws with random fluxes were obtained by Mishra [3]. The statistics of the random entropy solution such as the mean, variance and higher moments can be obtained. We will be interested in finding mean and variance in our numerical experiments.

Definition 3.4. The expectation of the random solution is defined by the formula

$$\mathbb{E}[U](x,t) = \int_{\Omega} U(x,t,\omega)\mathbb{P}(d\omega) = \int_{\mathbb{R}} U(x,t,y)\rho(y)dy$$

where $\rho(y)$ is essentially bounded probability density function which satisfies

$$\rho(y) = \frac{d\mathbb{P}(\omega)}{dy} \in (L^1 \cup L^\infty)(\mathbb{R}) \quad \textit{and} \quad \mathbb{P}(\mathbb{R}) = \int_{\mathbb{R}} \rho(y)dy = 1$$

also has the corresponding distribution function defined as

$$P(x) = \mathbb{P}(y \leq x) = \int_{-\infty}^{x} \rho(y)dy$$

The *variance* of the random solution is defined as

$$\mathbb{V}[U] = \mathbb{E}[U - \mathbb{E}[U]^2] = \mathbb{E}[U^2] - (\mathbb{E}[U])^2$$

In the upcoming sections, assuming the underlying deterministic problem and random entropy solutions are well posed, some of the efficient algorithms to approximate random entropy solutions will be discussed. Before we do that, I would like to give basic details on Karhunen-Loève expansion which is used to express random fields.

3.1.1 Karhunen-Loève expansion

A very common representation of random fields is to express them in terms of a infinite set of random variables. An efficient way to define initial parametrizations is in terms of a Karhunen-Loève expansion. Let's consider a random field $U : \Omega \mapsto L^2(D)$ for some domain $D \subset \mathbb{R}^d$ and suppose that $\mathbb{E}(U) = 0$. Then, the covariance function of this random field is defined as [3]

$$C_U \in L^2(D \times D) : \; C_U(x,y) = \mathbb{E}(U(x,\omega)U(y,\omega))$$

The corresponding covariance operator is defined as

$$K_C : L^2(D) \mapsto L^2(D) : K_C[g](x) := \int_D C_U(x,y)g(y)dy$$

The eigenvalues and eigenfunctions are denoted by λ_k and U_k

$$K_C[U_k] = \lambda_k U_k$$

The underlying random field U can be written as

$$U(x,\omega) = \sum_{k=1}^{\infty} Y_k(\omega)U_k(x)$$

The random variables Y_k are uncorrelated as

$$\mathbb{E}(Y_j Y_k) = \lambda_k \delta_{jk}$$

The random field u can be written in terms of its Karhunen-Loève expansion as

$$U = \bar{U} + \sum_{k=1}^{\infty} \sqrt{\lambda_k} Y_k U_k$$

where $\bar{U}$ is the mean value of the random field. Karhunen-Loève expansion can be truncated with finitely many terms M. The size of M depends on the rate of decay of the eigenvalues. The final statistics input can be written in terms of finite number of independent random parameters [3].

Proposition 3.1. *Consider the scalar stochastic Burger's equation*

$$U_t + [F(U,\omega)]_x = 0$$

$$U(x,0) = U_0(x),\ x \in [0,L]$$

with

$$F(U,\omega) = \frac{U^2}{2} + \sum_{j=1}^{\infty} \sqrt{\lambda_k} Y_j(\omega)\Phi_j(U)$$

where $\Phi_j(U)$ *and* λ_j *are the eigenfunctions and eigenvalues of*

$$\int_D C_Y(U_1,U_2)\Phi(U_1)dU_1 = \lambda\Phi(U_2)$$

If we use Gaussian process to describe the deviation from the Burgers flux $u^2/2$ *in the random flux* $F(U,\omega)$ *,and let* $Y(\omega) \in \mathcal{N}[0,1]$*, with exponential covariance [14]*

$$C_Y(U_1,U_2) = \sigma_Y^2 e^{-|U1-U2|/\eta}$$

then,

$$\lambda_j = \frac{2\eta\sigma_Y^2}{\eta^2\omega_j^2+1}, \quad \Phi_j(U) = \frac{\eta\omega_j\cos(\omega_j U) + \sin(\omega_j U)}{\sqrt{(\eta^2\omega_j^2+1)L/2+\eta}}$$

where ω_j *are the roots of*

$$(\eta^2\omega_j^2 - 1)\sin(\omega L) = 2\eta\omega\cos(\omega L)$$

Now assuming that unique random entropy solutions for the system (3.1) exists, I will present Monte Carlo Finite Volume Method and Stochastic Finite Volume Method to solve random conservation laws.

3.2 Monte Carlo Finite Volume Method

It is aimed to design an efficient Monte-Carlo type scheme for approximating random conservation law (3.1). Mischra and Schwab designed Monte-Carlo Finite Volume Method using spatial-temporal discretization of finite volume schemes [9].

Let the time step be $\Delta t > 0$ and the partition of the spatial domain $D \subset \mathbb{R}^d$ into a finite set of nonoverlapping open sets be τ. Let $K \subset \mathbb{R}^d$ be the convex polyhedra with boundary being a finite union of plane faces. Defining $\Delta_{x_K} := diamK$ and by $\Delta x(\tau) := \max \{ \Delta_{x_K} : K \in \tau \}$ the mesh width of τ, for any volume $K \in \tau$, the set $N(K)$ of neighboring volumes is defined

$$N(K) := \{K' \in \tau : K' \neq K \wedge meas_{d-1}(\bar{K} \cap \bar{K'}) > 0\}$$

For every $K \in \tau$ and $K' \in N(K)$ $v_{K',K}$ to be the unit normal pointing outward from the volume K at the face $\bar{K} \cap \bar{K'}$. We shall set

$$\lambda = \frac{\Delta t}{\min\{\Delta x_K : K \in \tau\}}$$

with the assumption of a uniform discretization in time with time step Δt.

When Monte Carlo Finite Volume Method is implemented, we will need to use the first-order finite volumes covered in Chapter 2 to approximate deterministic conservation law (1.1)

$$U_K^{n+1} = U_K^n - \frac{\Delta t}{meas(K)} \sum_{K' \in N(K)} F(U_K^n, U_{K+1}^n)$$

where

$$U_K^n \approx \frac{1}{meas(K)} \int_K U(x, t^n) dx$$

is an approximation to the cell average of the solution and F is the numerical flux. We have seen that numerical fluxes are obtained solving Riemann problems at each cell edge. Since Godunov and Engquist-Osher gave us the best results in terms of capturing shocks in the solution, I have prefarably used Engquist-Osher method as Riemann solver in Monte Carlo Algorithm.

MCFVM algorithm for the scalar conservation law problem with random initial data consists of the following four steps:

1. **Sample:** Given M independent, identically distributed samples U_0^i , $i = 1, .., M$ of random initial data

2. **Solve:** Solve the deterministic Burger's equation for each sample using a Finite Volume Method, i.e. Godunov or Engquist-Osher.

3. **Record:** Record the solution $U_K^{i,n}$

4. **Compute:** The expectation of the random solution field is estimated by the sample average of the approximate solution [3]:

$$E_M[U_\tau^n] := \frac{1}{M} \sum_{i=1}^{M} U_\tau^{i,n}$$

where

$$U_\tau^{i,n}(x) = U_K^{i,n}, \ \forall x \in K$$

Here, we should note that in step 2, any standard finite volume scheme can be used. Hence, existing code for FVM can be used and there is no need to rewrite FVM code. The following example is an implementation of Monte Carlo Finie Volume Method.

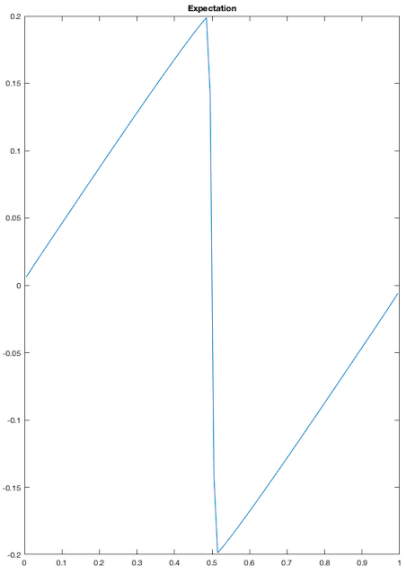

Figure 3.1: The expectation for Example 3.1 with Monte-Carlo FVM

Example 3.1. Consider the Burger's equation

$$U_t + (\frac{U^2}{2})_x = 0$$

with the initial condition having an uncertain amplitude:

$$U_0(x, \omega) = Y(\omega) \sin(2\pi x)$$

where $Y(\omega)$ is uniformly distributed, i.e. $Y(\omega) \in \mathcal{U}[0, 1]$

Figure (3.1) illustrates the numerical expectation . The smoothness of probability density function has no effect on shock. We can clearly expect the shock formation at $x = 0.5$ in the physical space. It also can be seen in the Figure (3.2) as the deviations go up nearby the shock.

Example 3.2. The second implementation is the Burger's equation with Riemann problem

$$U_t + (\frac{U^2}{2})_x = 0$$

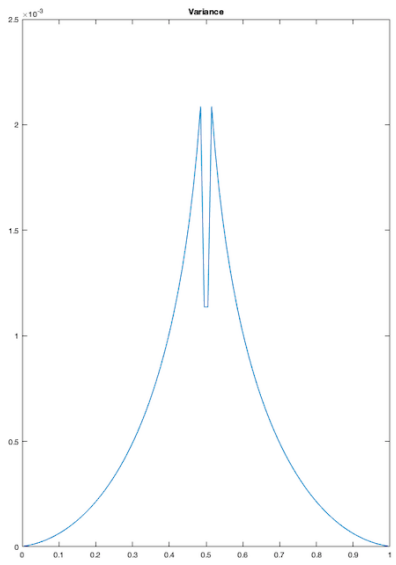

Figure 3.2: The variance for Example 3.1 with Monte-Carlo FVM

with

$$U_0(x,\omega) = \begin{cases} 2, & x < 1 + 0.1(2Y(\omega) - 1); \\ 1, & x > 1 + 0.1(2Y(\omega) - 1); \end{cases}$$

where $Y(\omega) \in \mathcal{U}[0,1]$. The problem can be interpreted as to find initial shock location and where the shock wave moves to right after the start. We can see where to expect the initial shock at the time step $t = 0.2$ in the Figure (3.3) It can be verified that the shock is nearby $x = 1.3$ as the deviation blows.

3.2.1 Error Bound for MCFVM

Mishra and Schwab have addressed the error bound for $E_M[U_\tau^n]$ to the mean $\mathbb{E}(U)$ [13].

Theorem 3.1. *Assume that*

$$U_0 \in L^\infty(\Omega, L^1(\mathbb{R}^d))$$

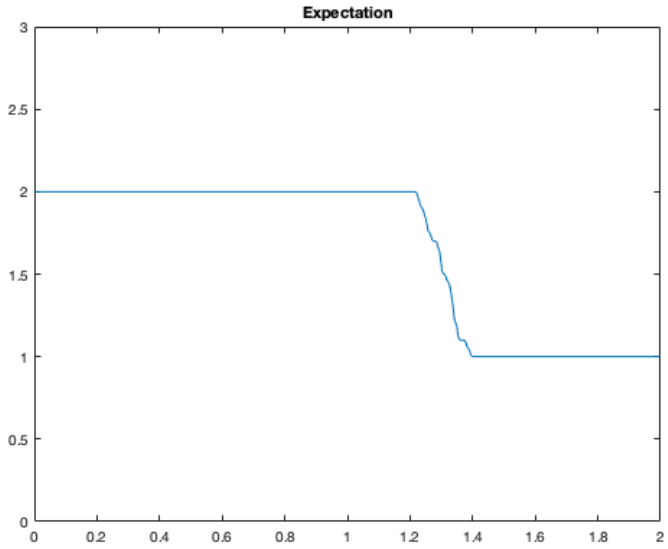

Figure 3.3: The expectation for Example 3.2 with Monte-Carlo FVM

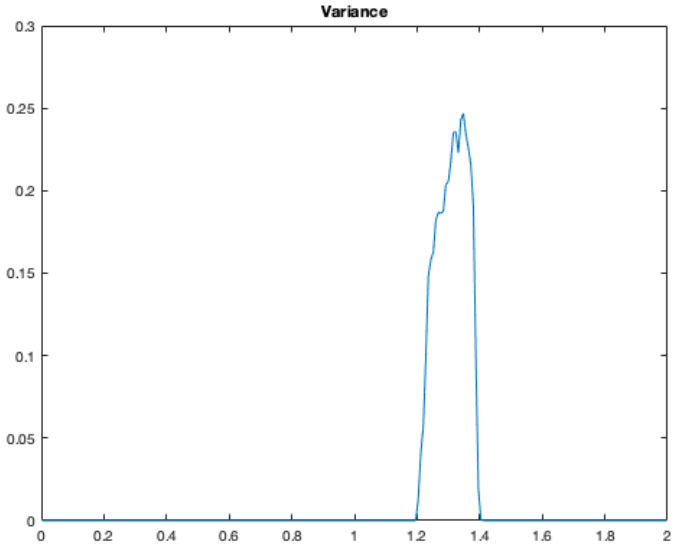

Figure 3.4: The variance for Example 3.2 with Monte-Carlo FVM

and that (3.2) for $m = 1$ is satisfied. Assuming further that we're using a finite volume method satisfying $\lambda = \frac{\Delta t}{\Delta x(\tau)}$ and for any initial data $U_0(x) \in L^1(\mathbb{R}^d)$ finite volume method approximation by the cell averages is defined

$$U_K^0 = \frac{1}{|K|}\int_K U_0(x)dx, \quad K \in \tau$$

Let's suppose that the deterministic FVM solver converges at rate $s > 0$ in $L^\infty([0,T]; L^1(\mathbb{R}^d))$ for every $0 < T < \infty$. Then the Monte Carlo estimate $E_M[U_\tau(\cdot,t)]$, for every M, has the error bound

$$\begin{aligned}
&||\mathbb{E}(U(\cdot,t)) - E_M[U_\tau(\cdot,t;\omega)]||_{L^2(\Omega;L^1(\mathbb{R}^d))} \\
&\leq C\Big\{M^{-\frac{1}{2}}||U_0||_{L^2(\Omega;L^1(\mathbb{R}^d))} + ||U_0 - U_\tau^0||_{L^\infty(\Omega;L^1(\mathbb{R}^d))} + t\Delta t^s||TV(U_0(\cdot,\omega))||_{L^\infty(\Omega;d\mathbb{P})}\Big\} \quad (3.3)
\end{aligned}$$

where $C > 0$ is independent of M and Δt as $M \to \infty$ and $\lambda\Delta x = \Delta t \to 0$

Proof: For arbitrary $t > 0$,

$$\begin{aligned}
&||\mathbb{E}(U(\cdot,t)) - E_M[U_\tau(\cdot,t)]||_{L^2(\Omega;L^1(\mathbb{R}^d))} \leq \\
&||\mathbb{E}(U(\cdot,t)) - E_M[U(\cdot,t)]||_{L^2(\Omega;L^1(\mathbb{R}^d))} + ||E_M(U(\cdot,t))) - E_M[U_\tau(\cdot,t)]||_{L^2(\Omega;L^1(\mathbb{R}^d))} := I + II
\end{aligned}$$

The term I is bounded by $2M^{-\frac{1}{2}}||U_0||_{L^2(\Omega;L^1(\mathbb{R}^d))}$. The reader is referred to [13] for more details. For term II, the following assumption which holds true for many standard FVM-schemes will be made:

$$||U(\cdot,\bar{t}) - U_\tau(\cdot,\bar{t})||_{L^1(\mathbb{R}^d)} \leq ||U_0 - U_\tau^0||_{L^1(\mathbb{R}^d)} + C\bar{t}TV(U_0)\Delta t^s$$

where $C > 0$ independent of Δx and for every $\bar{t}$, $(\Delta t)^s \leq \bar{t} \leq T$. Hence, using this assumption and setting up triangle inequality an upper bound for term II can be obtained

$$
\begin{aligned}
II &= ||E_M(U(\cdot,t))) - E_M[U_\tau(\cdot,t)]||_{L^2(\Omega;L^1(\mathbb{R}^d))} = ||E_M[U(\cdot,t;\omega) - U_\tau(\cdot,t)]||_{L^2(\Omega;L^1(\mathbb{R}^d))} \\
&\leq \frac{1}{M}\sum_{i=1}^{M} ||U^i(\cdot,t;\omega) - U^i_\tau(\cdot,t;\omega)||_{L^2(\Omega;L^1(\mathbb{R}^d))} \\
&\leq ess\sup_{\omega\in\Omega} ||U(\cdot,t;\omega) - U_\tau(\cdot,t;\omega)||_{L^1(\mathbb{R}^d)} \\
&\leq C\Big\{ ||U_0 - U^0_\tau||_{L^\infty(\Omega;L^1(\mathbb{R}^d)} + t\Delta t^s ||TV(U_0(\cdot,\omega))||_{L^\infty(\Omega,d\mathbb{P})} \Big\}
\end{aligned}
$$

Hence,

$$
I + II \leq C\Big\{ M^{-\frac{1}{2}} ||U_0||_{L^2(\Omega;L^1(\mathbb{R}^d))} + ||U_0 - U^0_\tau||_{L^\infty(\Omega;L^1(\mathbb{R}^d))} + t\Delta t^s ||TV(U_0(\cdot,\omega))||_{L^\infty(\Omega;d\mathbb{P})} \Big\}
$$

3.2.2 Work Estimates of MCFVM

Assuming that the computational domain $D \subset \mathbb{R}^d$ is bounded and boundary conditions are indicated with ∂D. The work for one time step to solve deterministic conservation law is of order $O(\Delta x^{-d})$ [13],

$$
Work(\tau) = O(\Delta x^{-d-1}), \quad \lambda\Delta x = \Delta t \downarrow 0
$$

which implies that the work for computation of the Monte Carlo estimate $\mathbb{E}_M[U^n_\tau]$

$$
Work(M,\tau) = O(M\Delta x^{-d-1}), \quad \Delta t = \lambda\Delta x \downarrow 0
$$

so from (3.3) the convergence order can be attained in terms of work, by choosing $M = \Delta t^{-2s}$ and applying the CFL condition $\lambda = \frac{\Delta t}{\Delta x(\tau)}$,

$$
Work(\tau) = O(\Delta t^{-2s}\Delta x^{-d-1}) = O(\Delta x^{-d-1-2s})
$$

hence

$$||\mathbb{E}(U(\cdot,t)) - E_M[U_\tau(\cdot,t;\omega)]||_{L^2(\Omega;L^1(\mathbb{R}^d))} \leq C\Delta t^s \leq C(Work(\tau))^{\frac{s}{d+1+2s}}$$

3.3 Stochastic Finite Volume Method

Tokareva and Abgrall came up with a different method to handle the uncertainty (randomness) in conservation laws [1]. Let's assume that the probability space Ω is presented by the parametrized probability space Γ. We will parametrize all random inputs using the random variable $y = Y(\omega)$. If Γ is low-dimensional, we can sub-divide it into disjoint subregions

$$\Gamma = \bigcup_{j=1}^{N_y} K_y^j, \qquad K_y^j \cap K_y^{j'} = \emptyset.$$

Similarly, we subdivide the physical domain $D = \cup_{i=1}^{N_x} K_x^i$.

Assuming the existence of probability density function $\rho(y)$, we can denote the expectation of the exact solution u:

$$\mathbb{E}[u(x,t)] = \int_\Gamma u(x,t,y)\rho(y)dy$$

Now integrate the random conservation law

$$\begin{cases} u_t(x,t,y) + (f(u(x,t,y))_x = 0 \\ u(x,0,y) = u_0(x,y) \end{cases} \tag{3.4}$$

over each spatial and each stochastic cell, i.e.

$$\int_{K_y^j}\int_{K_x^i} u_t\rho(y)dxdy + \int_{K_y^j}\int_{K_x^i} f_x\rho(y)dxdy = 0 \tag{3.5}$$

Introducing the cell averages at the time $t = t^n$,

$$\bar{u}_{i,j}(t^n) = \frac{1}{|K_y^j||K_x^i|}\int_{K_y^j}\int_{K_x^i} u(x,t^n,y)\rho(y)dxdy \tag{3.6}$$

and

$$\bar{f}_{i,j}(t^n) = \frac{1}{|K_y^j|}\int_{K_y^j}\left[\int_{K_x^i} F(u_L(x,t^n,y),u_R(x,t^n,y),y)\right]\rho(y)dxdy \tag{3.7}$$

where F is Godunov approximation of the flux function f,

$$|K_y^j| = \int_{K_y^j}\rho(y)dy, \qquad |K_x^i| = \int_{K_x^i} 1dx.$$

(3.6) and (3.7) can be written as:

$$\bar{u}_{i,j}(t^n) = \frac{1}{|K_y^j||K_x^i|}\mathbb{E}\left[\int_{K_x^i} u(x,t^n,y)dx\right]$$

$$\bar{f}_{i,j}(t^n) = \frac{1}{|K_y^j||K_x^i|}\mathbb{E}\left[\int_{K_x^i} F(u_L,u_R,y)dx\right]$$

(3.5) becomes:

$$\frac{d(\bar{u}_{i,j})}{dt} + \frac{1}{|K_x^i|}\bar{f}_{i,j}(t) = 0$$

which evolves in time in 1-D space as:

$$u_{i,j}^{n+1} = u_{i,j}^n - \frac{\Delta t}{\Delta x}[\mathbb{E}(F(u_i^n,u_{i+1}^n)|K_y^j) - \mathbb{E}(F(u_{i-1}^n,u_i^n)|K_y^j)]$$

Proof:

$$\frac{d(\bar{u}_{i,j})}{dt} + \frac{1}{|K_x^i|}\bar{f}_{i,j}(t) = 0 \Rightarrow \frac{u_{i,j}^{n+1} - u_{i,j}^n}{\Delta t} = \frac{-\bar{f}_{i,j}(t)}{\Delta x}$$

$$\Rightarrow u_{i,j}^{n+1} = u_{i,j}^n - \frac{\Delta t}{\Delta x}\bar{f}_{i,j}(t)$$

$$\Rightarrow u_{i,j}^{n+1} = u_{i,j}^n - \frac{\Delta t}{\Delta x|K_y^j|}\int_{K_y^j}\left[\int_{K_x^i} F(u_L(x,t^n,y), u_R(x,t^n,y), y)\right]\rho(y)dxdy$$

$$\Rightarrow u_{i,j}^{n+1} = u_{i,j}^n - \frac{\Delta t}{\Delta x|K_y^j|}\int_{K_y^j}\left[F(u_i^n, u_{i+1}^n, y) - F(u_{i-1}^n, u_i^n, y)\right]\rho(y)dy$$

$$\Rightarrow u_{i,j}^{n+1} = u_{i,j}^n - \frac{\Delta t}{\Delta x|K_y^j|}[\mathbb{E}(F(u_i^n, u_{i+1}^n)) - \mathbb{E}(F(u_{i-1}^n, u_i^n))]$$

$$\Rightarrow u_{i,j}^{n+1} = u_{i,j}^n - \frac{\Delta t}{\Delta x}[\mathbb{E}(F(u_i^n, u_{i+1}^n)|K_y^j) - \mathbb{E}(F(u_{i-1}^n, u_i^n)|K_y^j)]$$

This can be interpreted as the conditional expectation satisfying conservation law, hence we can state the following proposition.

Proposition 3.2. *Stochastic Finite Volume Method is conservative, that is,*

$$\sum_{i=1}\sum_{j=1} u_{i,j}^{n+1} = \sum_{i=1}\sum_{j=1} u_{i,j}^n - \frac{\Delta t}{\Delta x}\sum_{i=1}\sum_{j=1}\Big(\mathbb{E}(F(u_i^n, u_{i+1}^n)|K_j^y) - \mathbb{E}(F(u_{i-1}^n, u_i^n)|K_j^y)\Big)$$

The expectation can now be reconstructed by using the law of total expectation.

$$\begin{aligned}\mathbb{E}[u(x_i,t_n)] &= \sum_{j=1}^{N_y}\mathbb{E}[u(x_i,t_n)|y\in K_y^j]\mathbb{P}(y\in K_y^j)\\ &\approx \sum_{j=1}^{N_y} u_{i,j}^n|K_y^j|\end{aligned}$$

We can present the algorithm for Stochastic Finite Volume Method for random initial data as follows:

Algorithm 1 SFVM

procedure SFVM

Compute $|K_y^j| = \int \rho(K_y^j)$ for $j = 1, 2, ..., N$

Compute $u_{i,j}^0 = \frac{1}{|K_y^j|} \sum_{m=1}^{q} u_0(x, y_m)\rho(y_m)w_m$

Compute $F_{i+1/2}^n = F^n(u_i, u_{i+1})$ (Godunov)

$u_{j+1,i}^n \to u_{j,i}^n - \frac{\Delta t}{\Delta x}(F_{i+1/2}^n - F_{i-1/2}^n)$

$u_{i,j}^{n+1} \to u_{i,j}^n$

$\mathbb{E}(u_{i,j}^n) = \sum_{j=1}^{N} u_{i,j}^n |K_y^j|$

end procedure

where w_m is the weight and y_m is the node of quadrature rule, i.e. trapezoidal quadrature rule to calculate $\int u_0\rho(y)dy$ and q is the number of nodes/weights.

Example 3.3. Consider Burgers' equation with random initial condition:

$$\begin{cases} u_t + (\frac{u^2}{2})_x = 0 \ , x \in [0, 2\pi] \\ u(x, 0, y) = |y| \sin(2x - y) \end{cases}$$

with periodic boundary conditions and random variable y with density

$$\rho(y) = \frac{1}{0.65} \begin{cases} 0.1 \ , \ -1 \leq y \leq 0.5 \\ 1 \ , \ 0.5 \leq y \leq 1 \\ 0 \ , \ \text{otherwise} \end{cases}$$

Figure (3.5) shows the expected value of approximation of random solution over the spatial domain at the time step $t = 2.5$. We can expect the obvious shock formations in the solution at $x = 2$ and $x = 5$.

From the Figure (3.6) we can see the expected value of the approximate solution at different time steps.

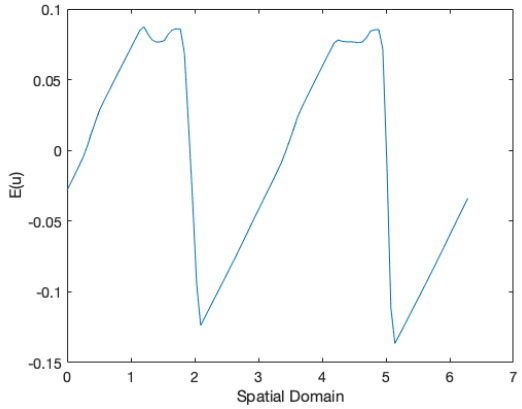

Figure 3.5: The expectation for Example 3.3 with SFVM at t=2.5

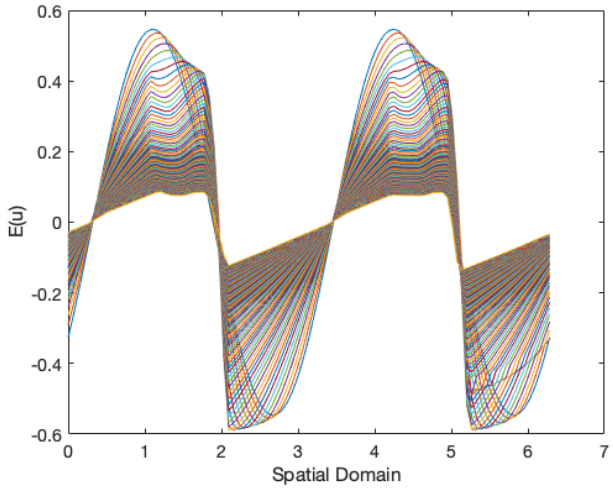

Figure 3.6: The expectation at different time steps

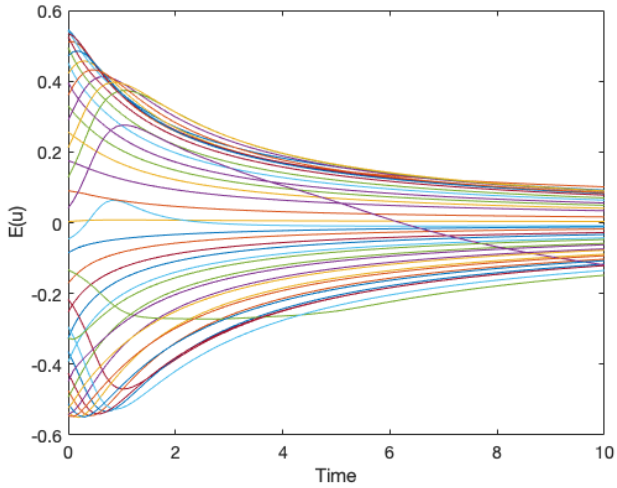

Figure 3.7: The expectation at different spatial nodes

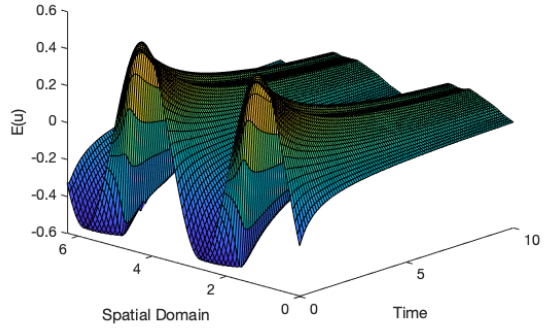

Figure 3.8: The distribution of expectation over time and spatial domain

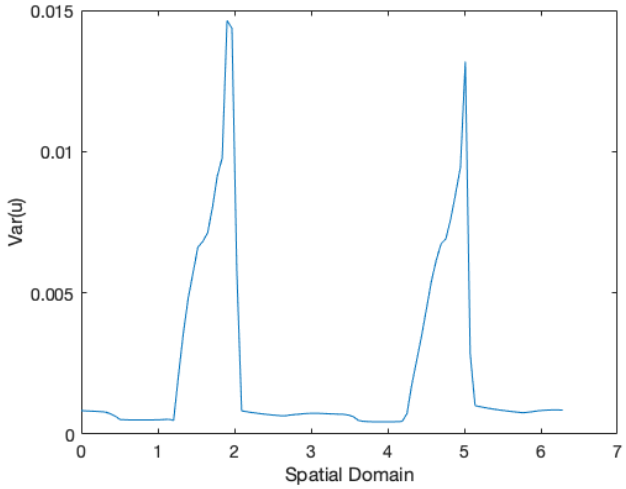

Figure 3.9: The variance at t=2.5

Figure (3.7) demonstrates the distribution of expectation at spatial nodes over the time. Each curve represents how expected value is distributed at a certain point in spatial domain over time.

The distribution of expected value of numerical solution can be seen in Figure (3.8).

The variance of the numerical solution can be seen in (3.9). We can verify the shock formations we observe at the expectation plot at $x = 2$ and $x = 5$. The deviations go up nearby the shock.

3.3.1 Convergence Analysis of SFVM

The error estimates for SFVM have been shown by Tokareva [14]

Estimates in L^∞ norm

Assume that $u(x,t,y)$ is exact solution to (3.4) and u_{ij}^n is its approximation at $t = t^n$ from SFVM. Assuming further that

$$||u - u_{ij}^n||_{L^\infty(DX\Gamma)} \leq C_1 \Delta x^p + C_2 \Delta y^r \tag{3.8}$$

where p and r are the convergence rates of the approximate solution by SFVM in physical and stochastic variable.

- Error estimate for the mean

  The mean value of exact solution at (x_i, t^n) is

  $$\mathbb{E}[u](x_i, t^n) = \int_\Gamma u(x_i, t^n, y)\rho(y)dy$$

  The mean value of approximate solution by SFVM at (x_i, t^n)

  $$E[u_{ij}^n](x_i, t^n) = \sum_{j=1}^{N_y} u_{ij}^n |K_y^j|$$

  Then we have [14]

$$
\begin{aligned}
|\mathbb{E}[u](x_i,t^n) - E[u_{ij}^n](x_i,t^n)| &= \Big| \int_\Gamma u(x_i,t^n,y)\rho(y)dy - \sum_{j=1}^{N_y} u_{ij}^n |K_y^j| \Big| \\
&= \Big| \sum_{j=1}^{N_y} \int_{K_y^j} u(x_i,t^n,y)\rho(y)dy - \sum_{j=1}^{N_y} u_{ij}^n \int_{K_y^j} \rho(y)dy \Big| \\
&= \Big| \sum_{j=1}^{N_y} \int_{K_y^j} \Big[u(x_i,t^n,y) - u_{ij}^n \Big] \rho(y)dy \Big| \\
&\leq \sum_{j=1}^{N_y} \int_{K_y^j} |u(x_i,t^n,y) - u_{ij}^n| \rho(y)dy \\
&\leq \sup_{K_y^j} |u(x_i,t^n,y) - u_{ij}^n| \sum_{j=1}^{N_y} \int_{K_y^j} \rho(y)dy \\
&= \sup_{K_y^j} |u(x_i,t^n,y) - u_{ij}^n| \int_\Gamma \rho(y)dy
\end{aligned}
$$

Using the property of probability density function $\int_\Gamma \rho(y)dy = 1$, we get

$$
|\mathbb{E}[u] - E[u_{ij}^n]| \leq ||u - u_{ij}^n||_{L^\infty(DX\Gamma)}
$$

- Error estimate for the variance

The variance of the exact solution at (x^i, t^n) is

$$
\mathbb{V}[u](x_i,t^n) = \mathbb{E}[(u(x_i,t^n) - \mathbb{E}[u](x_i,t^n))^2] = \mathbb{E}[u^2(x_i,t^n)] - (\mathbb{E}[u](x_i,t^n))^2
$$

and is approximated by

$$
V(u_{ij}^n) = E([u_{ij}^n]^2) - (E[u_{ij}^n])^2
$$

The error estimate can be obtained as [14]

$$
\begin{aligned}
||\mathbb{V}[u] - V(u_{ij}^n)||_{L^\infty(D)} &= ||\mathbb{E}[u^2(x_i,t^n)] - (\mathbb{E}[u](x_i,t^n))^2 - E([u_{ij}^n]^2) + (E[u_{ij}^n])^2||_{L^\infty(D)} \\
&= ||(\mathbb{E}[u^2(x_i,t^n)] - E([u_{ij}^n]^2)) - (\mathbb{E}[u](x_i,t^n))^2 - (E[u_{ij}^n])^2)||_{L^\infty(D)} \\
&\leq ||(\mathbb{E}[u^2(x_i,t^n)] - E([u_{ij}^n]^2))||_{L^\infty(D)} + ||\mathbb{E}[u](x_i,t^n))^2 - (E[u_{ij}^n])^2)||_{L^\infty(D)} \\
&= I + II
\end{aligned}
$$

I can be estimated by

$$
\begin{aligned}
|\mathbb{E}[u](x_i,t^n))^2 - (E[u_{ij}^n])^2)| &= \Big| \int_\Gamma u^2(x_i,t^n,y)\rho(y)dy - \sum_{j=1}^{N_y} (u_{ij}^n)^2 |K_y^j| \Big| \\
&= \Big| \sum_{j=1}^{N_y} \int_{K_y^j} u(x_i,t^n,y)^2\rho(y)dy - \sum_{j=1}^{N_y} (u_{ij}^n)^2 \int_{K_y^j} \rho(y)dy \Big| \\
&= \Big| \sum_{j=1}^{N_y} \int_{K_y^j} \Big[u^2(x_i,t^n,y) - (u_{ij}^n)^2 \Big] \rho(y)dy \Big| \\
&= \Big| \sum_{j=1}^{N_y} \int_{K_y^j} \Big[u(x_i,t^n,y) - (u_{ij}^n) \Big] \sqrt{\rho(y)} \Big[u(x_i,t^n,y) + (u_{ij}^n) \Big] \sqrt{\rho(y)} dy \Big| \\
&\leq \Big| \sum_{j=1}^{N_y} \Big(\int_{K_y^j} \Big[u(x_i,t^n,y) - (u_{ij}^n) \Big]^2 \rho(y)dy \Big)^{1/2} \Big(\int_{K_y^j} \Big[u(x_i,t^n,y) + (u_{ij}^n) \Big]^2 \rho(y)dy \Big)^{1/2} \Big| \\
&\leq C \Big| \sum_{j=1}^{N_y} \Big(\int_{K_y^j} \Big[u(x_i,t^n,y) - (u_{ij}^n) \Big]^2 \rho(y)dy \Big)^{1/2} \Big| \\
&\leq C \sum_{j=1}^{N_y} \Big(\int_{K_y^j} \Big| u(x_i,t^n,y) - (u_{ij}^n) \Big|^2 \rho(y)dy \Big)^{1/2} \\
&\leq C \sup_{K_y^j} |u(x_i,t^n,y) - (u_{ij}^n)| \Big(\int_{K_y^j} \rho(y)dy \Big)^{1/2} = C \sup_{K_y^j} |u(x_i,t^n,y) - (u_{ij}^n)|
\end{aligned}
$$

Therefore,

$$
||\mathbb{E}[u](x_i,t^n))^2 - (E[u_{ij}^n])^2)||_{L^\infty(D)} \leq C||u - u_{ij}^n||_{L^\infty(D)}
$$

To find an upper bound for term II

$$
\begin{aligned}
||\mathbb{E}[u](x_i,t^n))^2 - (E[u_{ij}^n])^2)||_{L^\infty(D)} = & \\
& \Big\| \Big(\mathbb{E}[u](x_i,t^n)) - (E[u_{ij}^n])\Big)\Big(\mathbb{E}[u](x_i,t^n)) + (E[u_{ij}^n])\Big) \Big\|_{L^\infty(D)} \\
& \leq \| \Big(\mathbb{E}[u](x_i,t^n)) - (E[u_{ij}^n])\Big) \|_{L^\infty(D)} \| \Big(\mathbb{E}[u](x_i,t^n)) + (E[u_{ij}^n])\Big) \|_{L^\infty(D)} \\
& \leq C \| \Big(\mathbb{E}[u](x_i,t^n)) - (E[u_{ij}^n])\Big) \|_{L^\infty(D)} || \\
& \leq C||u - u_{ij}^n||_{L^\infty(DX\Gamma)}
\end{aligned}
$$

It reveals that

$$||\mathbb{V}[u] - V(u_{ij}^n)||_{L^\infty(D)}|| \leq C||u - u_{ij}^n||_{L^\infty(DX\Gamma)}$$

Similar estimates in L^∞ can be obtained for higher moments.

Estimates in L^1 norm

Denoting the exact solution of (3.4) by u, the numerical solution which is exact in x variable and discretized in y by u_j^n ,assuming that the numerical solution $u_{i,j}^n$ converges with rate p in x variable and with rate r in y variable,

$$||u_j^n - u_{ij}^n||_{L^1(D)} \leq C_1 \Delta x^p$$
$$||u - u_j^n||_{L^1(\Gamma)} \leq C_2 \Delta y^r$$

hence,

$$||u - u_{ij}^n||_{L^1(DX\Gamma)} \leq C_1 \Delta x^p + C_2 \Delta y^r$$

- Error estimate for the mean

As before, the mean value of exact solution at (x_i, t^n) is a deterministic function

$$\mathbb{E}[u](x_i,t^n) = \int_\Gamma u(x_i,t^n,y)\rho(y)dy$$

and its approximation by SFVM at (x_i, t^n)

$$E[u_{ij}^n](x_i,t^n) = \sum_{j=1}^{N_y} u_{ij}^n |K_y^j| = \sum_{j=1}^{N_y} u_{i,j}^n \int_{K_y^j} \rho(y)dy = \int_\Gamma u_{ij}^n \rho(y)dy \ = \mathbb{E}[u_{ij}^n](x_i,t^n)$$

Then [14],

$$\begin{aligned}
||\mathbb{E}[u] - \mathbb{E}[u_{i,j}^n]||_{L^1(D)} &= ||\mathbb{E}[u] - \mathbb{E}[u_j^n] + \mathbb{E}[u_j^n] - \mathbb{E}[u_{i,j}^n]||_{L^1(D)} \\
&\leq ||\mathbb{E}[u] - \mathbb{E}[u_j^n]||_{L^1(D)} + ||\mathbb{E}[u_j^n] - \mathbb{E}[u_{i,j}^n]||_{L^1(D)} \\
&= \int_D |\mathbb{E}[u] - \mathbb{E}[u_j^n]|dx + \int_D |\mathbb{E}[u_j^n] - \mathbb{E}[u_{i,j}^n]|dx \\
&= \int_D \Big| \int_\Gamma (u - u_j^n)\rho(y)dy \Big| dx + \int_D \Big| \int_\Gamma (u_j^n - u_{ij}^n)\rho(y)dy \Big| dx \\
&\leq \int_D \int_\Gamma |(u - u_j^n)|\rho(y)dydx + \int_D \int_\Gamma |u_j^n - u_{ij}^n|\rho(y)dydx \qquad = I + II
\end{aligned}$$

I can be estimated as

$$\int_D \int_\Gamma |(u - u_j^n)|\rho(y)dydx \leq \int_D \sup_\Gamma \rho(y)dy \int_\Gamma |u - u_j^n|dydx = C|u - u_j^n|_{L^1(\Gamma)} \leq C\Delta y^r$$

and II is bounded by

$$\begin{aligned}
\int_D \int_\Gamma |u_j^n - u_{ij}^n|\rho(y)dydx &= \int_\Gamma \Big[\int_D |u_j^n - u_{ij}^n|dx \Big] \rho(y)dy \\
&= ||u_j^n - u_{ij}^n||_{L^1(D)} \int_\Gamma \rho(y)dy = ||u_j^n - u_{ij}^n||_{L^1(D)} \leq C\Delta x^p
\end{aligned}$$

It turns out the same convergence rate as (3.8) can be obtained for expectation.

$$||\mathbb{E}[u] - \mathbb{E}[u_{i,j}^n]||_{L^1(D)} \leq C_1\Delta x^p + C_2\Delta y^r \tag{3.9}$$

- Error estimate for the variance

As before, the variance of the exact solution at (x_i, t^n) is

$$\mathbb{V}[u](x_i,t^n) = \mathbb{E}[(u(x_i,t^n) - \mathbb{E}[u](x_i,t^n))^2] = \mathbb{E}[u^2(x_i,t^n)] - (\mathbb{E}[u](x_i,t^n))^2$$

and is approximated by

$$V(u_{ij}^n) = E([u_{ij}^n]^2) - (E[u_{ij}^n])^2 = \mathbb{E}([u_{ij}^n]^2) - (\mathbb{E}[u_{ij}^n])^2$$

Then [14],

$$\begin{aligned}||\mathbb{V}[u] - \mathbb{V}[u_{i,j}^n]||_{L^1(D)} &= ||\mathbb{E}[u^2] - (\mathbb{E}[u])^2 - \mathbb{E}[(u_{ij}^n)^2] + \mathbb{E}[(u_{ij}^n)^2]||_{L^1(D)} \\ &\leq ||\mathbb{E}[u^2] - \mathbb{E}[(u_{ij}^n)^2]||_{L^1(D)} + ||\mathbb{E}[u])^2 - \mathbb{E}[u_{i,j}^n]^2||_{L^1(D)} = I + II\end{aligned}$$

To estimate I

$$\begin{aligned}||\mathbb{E}[u^2] - \mathbb{E}[(u_{ij}^n)^2]||_{L^1(D)} &= \int_D |\mathbb{E}[u^2] - \mathbb{E}[(u_{ij}^n)^2]|dx \\ &= \int_D \Big| \int_\Gamma [u^2 - (u_{ij}^n)^2]\rho(y)dy\Big|dx \leq \int_D \int_\Gamma |u^2 - (u_{ij}^n)^2|\rho(y)dydx \\ &= \int_D \int_\Gamma |u - u_{ij}^n||u + u_{ij}^n|\rho(y)dydx \leq C\int_D \int_\Gamma |u - u_{ij}^n|dydx \\ &= C||u - u_{ij}^n||_{L^1(DX\Gamma)} \leq C\Delta x^p + D\Delta y^r\end{aligned}$$

and for II

$$\begin{aligned}||\mathbb{E}[u])^2 - (\mathbb{E}[u_{i,j}^n])^2||_{L^1(D)} &= \int_D |(\mathbb{E}[u])^2 - (\mathbb{E}[u_{i,j}^n])^2|dx \\ &= \int_D |\mathbb{E}[u] - \mathbb{E}[u_{i,j}^n||\mathbb{E}[u] + \mathbb{E}[u_{i,j}^n|dx \\ &\leq C||\mathbb{E}[u] - \mathbb{E}[u_{i,j}^n]||_{L^1(D)} \leq E\Delta x^p + F\Delta y^r\end{aligned}$$

Therefore we can verify that the same convergence rate (3.8) holds true for variance

$$||\mathbb{V}[u] - \mathbb{V}[u_{i,j}^n]||_{L^1(D)} \leq C_1 \Delta x^p + C_2 \Delta y^r$$

3.3.2 Work Estimates of SFVM

From (3.9) we know that [14]

$$||\mathbb{E}[u] - \mathbb{E}[u_{i,j}^n]||_{L^1(D)} \leq C_1 \Delta x^p + C_2 \Delta y^r$$

where p and r are the convergence rates of the approximate solution by SFVM in physical and stochastic variable. Let $x \in \mathbb{R}^n$, $y \in \mathbb{R}^m$. Suppose that the CFL condition is satisfied, that is, $\Delta t = O(\Delta x)$. Then, the total work done in approximating the random solution u using SFVM [14]:

$$CN_xN_yN_t = C\frac{1}{\Delta x^n}\frac{1}{\Delta y^m}\frac{1}{\Delta t} = \frac{C}{\Delta x^{n+1}\Delta y^m} = C\Delta x^{-(n+1)}\Delta y^{-m}$$

Chapter 4

Conclusion/Future Work

We have studied the solutions of Burger's equation and implemented some methods in deterministic case. Godunov and Engquist-Osher schemes gave the best result in capturing the shocks of Burger's equation. Hence, we have preferred using these two schemes when we were doing simulations in random media. We used a particular Flux Limiter Method to solve Burger's equation. It was second order accurate in the space depending on the smoothness and convergent. To deal with uncertainty in conservation laws, we firstly used Monte Carlo FVM. Its convergence rate is very slow and this encouraged us to study Stochastic FVM. We analyzed Stochastic FVM and set up an algorithm for conservation laws with random initial data. We made an implementation and the scheme turned out to be conservative. Conservativeness leads to stability and convergence. The curse of dimensionality only allows Stochastic FVM to be viable for a small to moderate number of sources of uncertainty.

We plan to use SFVM as the first step to get a grasp on quantities of interest and hope to use this notion to develop adaptive schemes. Also, we want to do simulations for conservation laws with random flux. As mentioned in Chapter 1, shallow water equations is one of the applications of conservation laws. We aim to model shallow water equations and do simulations using Stochastic FVM.

Bibliography

[1] Tokareva S., Abgrall R., Stochastic Finite Volume Methods for computational uncertainty quantification in hyperbolic conservation laws

[2] Risebro N.H., Mishra S., Schwab C., Tokareva S., 2002. Numerical Solution of Scalar Conservation Laws with Random Flux Functions.

[3] Abgrall R., Mishra S., 2017. Handbook of Numerical Analysis, Vol. 18 p 507-544.

[4] Galiano S. J., Zapata M. U., 2010. A new TVD flux-limiter method for solving nonlinear hyperbolic equations.

[5] Mishra S., Fjordholm U.S., Abgrall R. Numerical Methods for Conservation Laws and Related Equations Notes

[6] LeVeque R.J., 1992. Numerical Methods for Conservation Laws, Birkhauser-Verlag, Basel.

[7] Poette G. , Despres B. , Lucor B. Uncertainty quantification for systems of conservation laws

[8] Xin, J.,2009. An Introduction to Fronts in Random Media.

[9] Schwab C. , Mishra S. , Šukys J. Multi-level Monte Carlo finite volume methods for uncertainty quantification of acoustic wave propagation in random heterogeneous layered medium.

[10] Ballou D., Solutions to Nonlinear Hyperbolic Cauchy Problems without Convexity Conditions, Transactions of the American Mathematical Society, 152, Dec. 1970, 441-460.

[11] Ostapenko V., Conservation laws of shallow water theory and the Galilean relativity principle, Journal of Applied and Industrial Mathematics 8(2):274-286 · April 2014

[12] Godunov S.K., A Difference Scheme for Numerical Solution of Discontinuous Solution of Hydrodynamic Equations. Math. Sbornik, 47:271306, 1959.

[13] Mishra S., Schwab C., 2012 Sparse tensor multi-level Monte Carlo finite volume methods for hyperbolic conservation laws with random initial data. Math. Comput. 81 (180), 1979-2018

[14] Tokareva S., Stochastic Finite Volume Methods for computational uncertainty quantification in hyperbolic conservation laws

[15] Abgrall R., 2008. A simple, flexible and generic deterministic approach to uncertainty quantification in non-linear problems. Inria. Tech. Report.

[16] LeVeque R. J., Finite volume methods for nonlinear elasticity in heterogeneous media, Int. Numer. Meth. Fluids, 40 (2002), pp.93-104

[17] LeVeque R. J., Wave propagation algorithms for multi-dimensional hyperbolic systems, J. Comput. Phys., 131 (1997), pp. 327–353.

[18] Roe P. L. Approximate Riemann solvers, parameter vectors, and difference schemes, J. Comput. Phys., 43 (1981), pp. 357–372.

[19] Crandall M. G., Majda A. Monotone difference approximations for scalar conservation laws,Math. Comp.,34 (1980),pp. 1–21.

[20] Godunov S.K. A finite difference method for the numerical computation of discontinuous solutions of the equations of fluid dynamics ,Math. USSR Sb.,47 (1959),pp. 271–290.

[21] Engquist B., Osher S., One sided difference approximations for nonlinear conservation laws,Math. Comp.,36 (1980),pp. 45–75.

[22] Lax P.D., Wendroff B., Systems of conservation laws,Comm. Pure Appl. Math.,23 (1960),pp. 217–237.

[23] Holden H., Risebro N. H. (2007) Front tracking for conservation laws. Second Corr. Printing, Springer Verlag, New York

[24] Bale D., LeVeque R.J., Mitran S., Rossmanith J. A wave-propagation method for conservation laws and balance laws with spatially varying flux functions. 2002, submitted (ftp://amath.washington.edu/pub/rjl/ papers/vcflux.ps.gz)

[25] Abgrall R., Congedo P., 2013. A semi-intrusive deterministic approach to uncertainty quantification in non-linear fluid flow problems. J. Comput. Phys. 235, 828–845.

[26] Ghanem R., Higdon D., Owhadi H. (Eds.), 2016. Handbook of Uncertainty Quantification. Springer, Heidelberg.

[27] Harten A., 1983. High-resolution schemes for hyperbolic conservation laws. J. Comput. Phys. 49, 357–393.

[28] Sukys J., 2014b. Robust Multi-level Monte Carlo Finite Volume Methods for Systems of Hyperbolic Conservation Laws With Random Input Data (Ph.D. thesis). ETH.

[29] Schwab C., Tokareva S., 2013. High order approximation of probabilistic shock profiles in hyperbolic conservation laws with uncertain initial data. M2AN Math. Model. Numer. Anal. 47, 807–835.

[30] Lin G., Su C.H., Karniadakis G.E., 2006. Predicting shock dynamics in the presence of uncertainties. J. Comput. Phys. 217, 260–276.

[31] Wan X., Karniadakis G.E., 2006. Long-term behaviour of polynomial chaos in stochastic flow simulations. Comput. Meth. Appl. Mech. Eng. 195, 5582–5596.

[32] Xiu D., Karniadakis G.E.. Modeling uncertainty in ow simulations via generalized polynomial chaos. J, Comp. Phys., 187 (2003), 137-167.

[33] Schwab C., Todor R.A. Karhunen-Loève approximation of random fields by generalized fast multipole methods. J. Comput. Phys., 217 (2006), 100-122.

[34] Risebro N.H., Schwab C., Weber F. Multilevel monte-carlo front tracking for random scalar conservation laws. SAM report 2012-17, http://www.sam.math.ethz.ch/reports/2012/17

[35] Poette G., Despres B., Lucor D. Uncertainty quantification for systems of conservation laws. J. Comp. Phys., 228 (2009), 2443-2467.

[36] Holden H., Risebro N.H. Conservation laws with a random source. Appl. Math. Optim., 36 (1997), 229-241.

[37] Ghanem R., Spanos P. Stochastic Finite Elements: A Spectral Approach. Dover, 2003.

[38] Barth A., Schwab C., Zollinger N. Multi-level Monte Carlo finite element method for elliptic PDEs with stochastic coeffcients. Numer. Math., 119 (2001), 123-161.

[39] Godlewski E., Raviart P.A. Numerical approximation of hyperbolic systems of conservation laws. Applied Mathematical Sciences, 118. Springer-Verlag, New York, 1996.

[40] Godlewski E., Raviart P. Hyperbolic systems of conservation laws. Ellipses Publ., Paris, 1995.

[41] Abgrall R., Congedo P.M., Geraci G., Rodio M.G., 2015. Stochastic discrete equation method (sDEM) for two phase flows. J. Comput. Phys. 299, 281–306.

[42] Abgrall R., Congedo P.M., Geraci G., 2014. A one-time truncate and encode multiresolution stochastic framework. J. Comput. Phys. 257 (A), 19–56.

[43] Barth, T.J., 2012. On the propagation of statistical model parameter uncertainty in CFD calculations. Theo. Comp. Fluid. Dynamics 26, 435–457.

[44] Barth, T.J., 2014. Non-intrusive uncertainty propagation with error bounds for conservation laws containing discontinuities. In: Uncertainty Quantification in Computational Fluid Dynamics. Lecture Notes in Computational Science and Engineering, vol. 92. Springer, Heidelberg, pp. 1–58.

[45] Fjordholm U.S., Kappeli R., Mishra S., Tadmor E., 2016a. Construction of approximate entropy measure-valued solutions for hyperbolic systems of conservation laws. J. Found. Comput.Math.

[46] Fjordholm U.S., Lanthaler S., Mishra S., 2016b. Statistical solutions of hyperbolic conservation laws I: foundations. Available from ArXiv:1605.05960.

[47] Ghanem R., Higdon D., Owhadi H. (Eds.), 2016. Handbook of Uncertainty Quantification. Springer, Heidelberg.

[48] Harten A., 1995. Multiresolution algorithms for the numerical solution of hyperbolic conservation laws. Comm. Pure Appl. Math. 48 (12), 1305–1342.

[49] Harten A., Engquist B., Osher S., Chakravarty S.R., 1987. Uniformly high order accurate essentially non-oscillatory schemes. J. Comput. Phys. 71, 231–303.

[50] Heinrich S., 2001. Multilevel Monte Carlo methods. In: Large-scale scientific computing. Third international conference LSSC 2001, Sozopol, Bulgaria Lecture Notes in Computer Science, vol. 2170. Springer-Verlag, Berlin, pp. 58–67.

[51] Muller F., 2014. Stochastic Methods for Uncertainty Quantification in Subsurface Flow and Transport Problems. ETH (Ph.D. thesis).

[52] Muller F., Jenny P., Meyer D.W., 2013. Multilevel Monte Carlo for two phase flow and Buckley-Leverett transport in random heterogeneous porous media. J. Comput. Phys. 250 (1), 685–702.

[53] Ma X., Zabaras N., 2009. An adaptive hierarchical sparse grid collocation algorithm for the solution of stochastic differential equations. J. Comput. Phys. 228, 3084–3113.

[54] Mishra S., Schwab C., Sukys J., 2012b. Multi-level Monte Carlo finite volume methods for shallow water equations with uncertain topography in multi-dimensions. SIAM J. Sci. Comput. 34 (6), B761–B784.

[55] Sukys J., 2014a. Adaptive load balancing for massively parallel multi-level Monte Carlo solvers. In: PPAM 2013, Part I, LNCS, vol. 8384. Springer, Heidelberg, pp. 47–56.

[56] Sukys J., Schwab C., Mishra S., 2013. Multi-level Monte Carlo finite difference and finite volume methods for stochastic linear hyperbolic systems. In: MCQMC 2012, Proceedings in Mathematics and Statistics. Springer, New York, pp. 649–666.

[57] Witteveen, J.A.S., Iaccarino G., 2013. Essentially non-oscillatory stencil selection and subcell resolution in uncertainty quantification. In: Uncertainty Quantification in Computational Fluid Dynamics, Lecture Notes in Computational Science and Engineering, vol. 92, Springer, Heidelberg, pp. 295–333.

[58] Yang X., Choi M., Lin G., Karniadakis G.E., 2012. Adaptive ANOVA decomposition of stochastic incompressible and compressible flows. J. Comput. Phys. 231, 1587–1614.

[59] Godlewski E., Raviart. P. Hyperbolic systems of conservation laws. Ellipses Publ., Paris, 1995.

[60] Kroner D. Numerical schemes for conservation laws. Wiley-Teubner Series Ad- vances in Numerical Mathematics. John Wiley and Sons Ltd., Chichester, 1997.

[61] LeVeque R.J. Finite volume methods for hyperbolic problems. Cambridge Texts in Applied Mathematics. Cambridge University Press, Cambridge, 2002.

[62] Lin G., Su C.H., Karniadakis G.E. Stochastic modelling of random roughness in shock scattering problems: theory and simulations. Comp. Meth. App. Mech. Eng., 197 (2008), 3420-3434.

[63] Wehr J., Xin J.. Front speed in the Burgers equation with a random ux. J.Statist. Phys., 88 (1997), 843-871.

[64] Shu C. W. TVB uniformly high order schemes for conservation laws. Math. Comp., 49 (1987), 105-121.

[65] Le Maitre O., Najm H., Ghanem R., Knio O. Multi-resolution analysis of Wienertype uncertainty propagation schemes. J. Comp. Phys., 197 (2004), 502-531.

[66] Barth A., Schwab C. and Zollinger N. Multilevel MC Method for Elliptic PDEs with Stochastic Coefficients. Report, SAM, 2010 (in review).

[67] Chan T. F., Golub. G. H. , LeVeque R. J. Updating Formulae and a Pairwise Algorithm for Computing Sample Variances. STAN-CS-79-773, 1979.

[68] Dafermos M. Hyperbolic Conservation Laws in Continuum Physics (2nd Ed.). Springer Verlag (2005).

[69] Giles M. Improved multilevel Monte Carlo convergence using the Milstein scheme. Preprint NA-06/22, Oxford computing lab, Oxford, U.K, 2006.

[70] Lin G., Su C.H., Karniadakis G. E. The stochastic piston problem. PNAS 101:15840-15845, 2004.